NHRP Contestable Research Project
A New Paradigm for Alpine Fault Paleoseismicity: The Northern Section of the Alpine Fault

R Langridge JD Howarth

GNS Science Miscellaneous Series 121
November 2018

GNS SCIENCE
TE PŪ AO

DISCLAIMER

The Institute of Geological and Nuclear Sciences Limited (GNS Science) and its funders give no warranties of any kind concerning the accuracy, completeness, timeliness or fitness for purpose of the contents of this report. GNS Science accepts no responsibility for any actions taken based on, or reliance placed on the contents of this report and GNS Science and its funders exclude to the full extent permitted by law liability for any loss, damage or expense, direct or indirect, and however caused, whether through negligence or otherwise, resulting from any person's or organisation's use of, or reliance on, the contents of this report.

BIBLIOGRAPHIC REFERENCE

Langridge, R.M., Howarth, J.D. 2018. A New Paradigm for Alpine Fault Paleoseismicity: The Northern Section of the Alpine Fault. Lower Hutt (NZ): GNS Science. 49 p. (GNS Science miscellaneous series 121). doi:10.21420/G2WS9H

RM Langridge, GNS Science, PO Box 30-368, Lower Hutt, New Zealand

JD Howarth, Dept. of Earth Sciences, Victoria University of Wellington, New Zealand

ISSN 1177-2441 (print)
ISSN 1172-2886 (online)
ISBN (print): 978-1-98-853079-6
ISBN (online): 978-1-98-853080-2
http://dx.doi.org/10.21420/G2WS9H

CONTENTS

FIGURES

TABLES

ABSTRACT

The 194 km long northern section of the Alpine Fault, as defined in the New Zealand national seismic hazard model (AlpineK2T fault source), runs from Lake Kaniere to Tophouse, near St Arnaud. This NHRP-funded project focuses on a paleo-earthquake record of the northern section, which is less well-established than that of the central and southern sections of the Alpine Fault. The new datasets collected as part of this project are: airborne lidar, on-fault paleoseismic trenches and a paleoseismic lake cores, along with an extensive program of radiocarbon dating. These data are used to develop precise records of the timing of past earthquakes that will indicate how they correlate along the length of the northern section.

Four new swaths of airborne LiDAR were acquired along the Alpine Fault between the Hokitika River and Lake Daniell. These swaths were used to map the fault in detail and to locate paleoseismic sites and small geomorphic offsets, e.g. horizontally offset channels and terrace risers that are used to characterise past earthquake slip at these sites.

On-fault paleoseismic trench studies were undertaken at the Maruia and Ahaura River sites. At the Maruia River (Calf Paddock) site two trenches were excavated across the fault in association with known offsets of river terrace risers. The results from these trenches indicate evidence for three paleoseismic events related to c. 12 m of dextral slip on the fault during the last c. 1250 years. A fourth paleoseismic event is inferred from initiation of a major degradation cycle of the river prior to Event III. Based on OxCal radiocarbon age modelling the most recent paleoseismic event (MRE) here occurred since AD 1492 and was associated with only c. 1.3 m of horizontal slip. These paleo-earthquake timing results are consistent with precisely-dated off-fault shaking evidence from turbidites in the sedimentary record of Lake Christabel which is located 6 km to the south in the hanging wall of the Alpine Fault. Trenching results from the Maruia River site indicate it has one of the longest on-fault paleoseismic records along the Alpine Fault with up to 4 paleoseismic events within the last 1800 years or less. The preliminary timings of the four events are: MRE – since AD 1492–1939, penultimate event – AD 1453–1596; Event III – AD 753–945; and a possible Event IV from AD 213–731. Three of these events are associated with single-event displacements, while the fourth is linked to a major geomorphic change at the site. While these four events have broad timing constraints, they correlate reasonably well with four major and well-dated shaking events recognised in cores from Lake Christabel.

Two paleoseismic trenches were excavated at the Ahaura River (Coates) site. The data from these trenches is still being analysed and results are preliminary. The Coates-1 trench was excavated at the site of a channel and riser related to an abandoned floodplain, offset dextrally by c. 10 ± 2 m. Relationships in the trench suggest that this displacement is associated with 2 or 3 paleo-earthquakes. Radiocarbon dating of units has provided equivocal results so far and requires more effort to develop paleoseismic event chronologies at the Coates site.

A data collection campaign including bathymetric and geophysical surveying, coring, and radiocarbon dating of sediments was undertaken at Lake Brunner, 10 km northwest of the Alpine Fault at Inchbonnie, with the goal of having another dataset of paleo-shaking along the northern section of the Alpine Fault to compare with other lakes (Kaniere, Christabel, Rotoiti) and to on-fault paleoseismic datasets. Five turbidite sequences recognised in cores and related to strong shaking of the lake basin, were recognised during the last c. 1500 years. Prior to this time the lake was impacted by fluvial deposition related to inflow of the

Taramakau River. The timing of the most recent shaking event (95% PDF) in the lake is between AD 1586 and AD 1751. The age model also constrains the timing of five additional MMI 9 events in Lake Brunner to AD ~1400, AD ~1125, AD ~925, AD ~550 and AD ~350.

In future, paleoseismic records from other on-fault and off-fault pairs, e.g. the Inchbonnie-Lake Brunner and Toaroha-Kaniere, will be assessed to:

1. match the timing and number of paleoseismic rupture events with shaking events at nearby lakes across strike;
2. consider whether both on-fault and off-fault records along strike can be used to assess the past lengths of Alpine Fault ruptures.

Outreach and stakeholder engagement were important parts of this project, including on-site field engagement with media, students, and the public, Project AF8 Civil Defence workshop talks, and an international conference field trip. Papers related to this project have been published (including a decadal review of the paleoseismicity of the Alpine Fault), and several conference presentations have been delivered.

The science learnings from this project are ongoing. However, results to date highlight the value of our combined on- and off-fault approach to researching the paleoseismicity of the Alpine Fault. In future we hope to develop conditional probability of fault failure statistics for sites along the northern section of the Alpine Fault.

KEYWORDS

Alpine Fault, paleoseismicity, northern section, Lake Brunner, Maruia River, Ahaura River

KEY MESSAGES FOR MEDIA

- The ‘northern section’ of the Alpine Fault runs from near Hokitika to the Nelson Lakes area and is considered a separate earthquake source to the more frequently described central and southern sections of the Alpine Fault.
- The past earthquake rupture history of the northern section is poorly understood compared to the rest of the Alpine Fault, warranting geologic studies to determine the timing of past earthquakes and past slip. The research approach was to pair up on-fault (trenching) studies with off-fault (lake) studies at key locations.
- New airborne LiDAR data was acquired to characterise the location of the fault and to aid in the discovery of paleoseismic trenching and displacement sites
- On-fault trench excavations were focused at the Maruia River and Ahaura River sites. The results from these trenches indicate evidence for three large earthquake events on the Alpine Fault there during the last c. 1250 years, accounting for c. 12 m of right-lateral slip. Based on OxCal radiocarbon age modelling the most recent paleoseismic event here occurred from since AD 1492 and before1840 and was associated with only c. 1.3 m of horizontal slip. At Ahaura, 2 trenches also revealed evidence for 3 past surface-rupturing earthquakes on the northern section of the Alpine Fault. Radiocarbon dates that will constrain the timing of these events are still pending form this site. An offset channel associated with one of the trenches suggests a single-event displacement range of 3 ± 1 m per event.
- A new lake-based coring study was undertaken at Lake Brunner to complement previous studies at lakes Christabel and Kaniere. The Lake Brunner record displays 5 major (MMI 9) earthquake shaking events in the last 1500 years, causing turbidite deposits to be deposited in the bottom of the lake. Prior to this the Taramakau River flowed into the lake, which precludes viewing a longer record of turbidites.
- In the future, on-fault and off-fault paleo-earthquake data will be combined to assess the recurrence interval of large earthquakes on the northern section, and whether they have variable surface displacement and rupture length. These data will allow us to estimate the probability of a large earthquake at several points along the fault.

1.0 INTRODUCTION

The Alpine Fault forms one of the largest seismic hazards in the South Island of New Zealand. Geologic studies of the central and southern parts of the fault have established that it generates very large (magnitude MW »7) to great (MW >8) earthquakes every few hundred years (Berryman et al., 2012a, b; Howarth et al., 2012). For the southern and central sections of the Alpine Fault the most recently published recurrence intervals for large to great earthquakes are c. 291 ± 23 years and 263 ± 68 years, respectively (Cochran et al., 2017; Howarth et al., 2016a), with the most recent faulting event having occurred in c. AD 1717.

The northern section of the Alpine Fault, which runs for c. 190 km from near Hokitika to the Nelson Lakes area (Figure 1.1), is fundamentally distinct in character to the central and southern sections of the Alpine Fault, due its relationship with the Marlborough Fault System – a more distributed part of the Australia-Pacific plate boundary (Langridge and Berryman, 2005; Wallace et al., 2007). While the New Zealand national seismic hazard model (NSHM; Stirling et al., 2012) identifies it as a separate earthquake source, the past earthquake history (timing, slip) of the northern section is rather poorly understood. New airborne LiDAR topographic data was acquired along four parts of the northern section, to characterise the location of the fault and to aid in the discovery of paleoseismic trenching and displacement sites. The latter is important as the distribution of surface displacement in past earthquakes can inform us about past earthquake magnitudes and rupture lengths (De Pascale et al., 2014).

In this study, new on-fault trench excavations were focused at the Maruia River and Ahaura River sites. The records from these sites are combined with results from other trench sites at the Toaroha and Kokatahi rivers, Inchbonnie and the Matakitaki River (Yetton and Wells, 2010; Yetton, 2002; Howarth et al., 2018; Langridge et al., in review) to produce a comprehensive record of the timing and displacement of the last few earthquakes. New lake coring studies have been undertaken as part of this project at Lake Brunner. Such studies at deep lakes along the Alpine Fault have provided new insights into the record of strong shaking, as observed by the presence and timing of deep water turbidite deposits and post-earthquake landscape response (Howarth et al., 2012, 2016a, b). Results from Lake Brunner will complement those previously garnered from lakes Kaniere, Christabel and Rotoiti, which all straddle the northern section of the Alpine Fault (Figure 1.1). In contrast to on-fault trench studies, lake-based paleoseismic studies along the Alpine Fault have produced precise paleo-earthquake timings from deposits rich in organic fragments that provide accurate radiocarbon dates of sediments and events (Howarth et al., 2012 2014). Precise paleo-earthquake timings allow for reasonable along-strike correlations of rupture events from site to site.

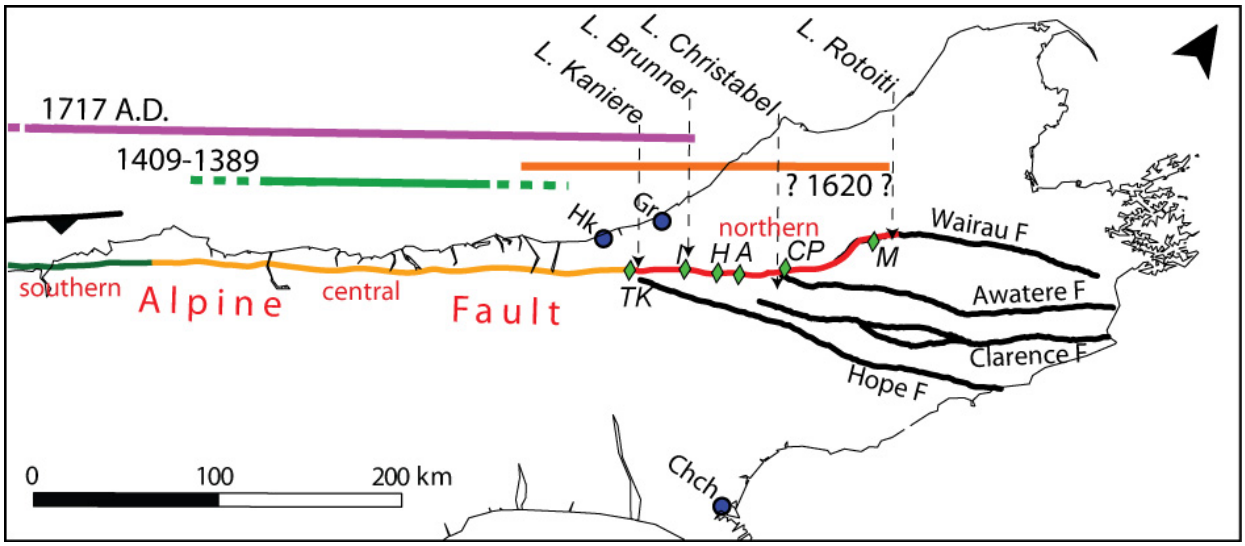

Figure 1.1 Space-time diagram of Alpine Fault ruptures (prior to this study), including sections of the fault, lake sites (italics, arrows) and trench sites (diamonds). Key towns and cities (Gr - Greymouth, Hk - Hokitika, Chch - Christchurch) are shown by blue circles. Trench sites are: TK - Toaroha/Kokatahi rivers; I - Inchbonnie; H - Haupiri River; A - Ahaura River; CP - Calf Paddock (Maruia); M - Matakitaki River. Current rupture models for the central-northern section transition have been revised by Howarth et al. (2018).

The project aimed to carry these results through into improved understandings of fault and earthquake behaviour for the northern section, and in relation to the entire Alpine Fault (e.g. Biasi et al., 2015; Howarth et al., 2016a, b). With time, results of on-fault and off-fault paleo-earthquake data will be combined to assess the continuity and rupture length of individual past earthquake ruptures, and the recurrence interval of large earthquakes on the northern section of the Alpine Fault. These outcomes will allow us to consider whether individual ruptures can have variable surface displacement and rupture length. New geologic data will also enable us to estimate the probability of a large earthquake at several points along the fault.

In light of the series of large earthquakes through the South Island during the last decade, our aim has also been to inform the public, science, civil defence and other stakeholders of our research as it progresses. From this, regional and district authorities would be better informed of seismic hazard and would therefore be empowered to make better planning decisions involving natural hazards. Therefore, in early 2019 we plan to coordinate a science talk tour with Project AF8, that takes in Ngati Waewae stakeholders at Arahura, West Coast Regional/Grey District Councils in Greymouth and Buller District Council in Westport.

Chapters in this report are laid out according to the key Research Aims of the project, beginning with the acquisition of airborne LiDAR and mapping outcomes (Chapter 2), collection of on-fault paleoseismic data (Chapter 3), collection of off-fault paleoseismic data (Chapter 4), development of robust paleo-earthquake chronologies and conditional probability estimates (Chapter 5), and engagement with stakeholders (Chapter 7). Chapter 8 contains a brief discussion of the science outcomes of the project.

2.0 RESEARCH AIM 1.1 — ACQUIRE NEW AIRBORNE LIDAR COVERAGE

"We will acquire airborne LiDAR strip data along the Alpine Fault and use these to map the fault and identify and measure fault displacements. Airborne LiDAR strip data (8 strips of c. 7 km length) will be acquired along the Alpine Fault between the Hokitika and Maruia rivers covering largely unforested areas with good access. We will use the data to develop high-quality DEMs and hill-shade models that can be used in a GIS to map the fault and identify and measure horizontal and vertical fault displacements."

2.1 LiDAR Acquisition

We proposed an extensive airborne LiDAR acquisition with the goal of capturing LIDAR along key strips of the northern section of the Alpine Fault. Four areas were selected to match with the allocated budget and cost. These areas were prioritised for locating sites where paleoseismic and slip rate studies could be undertaken, particularly in areas that had good road access and where preliminary geologic studies had already taken place.

Australian Aerial Mapping (AAM; formerly NZAM) were contracted to acquire the LiDAR data. LiDAR data was acquired in September 2015 with a Riegl Q1560 sensor, providing optimal coverage with which to develop detailed digital elevation (DEMs) and hill-shade models. Based on point coverage density and the underlying vegetation cover density we were able to develop 2-m quality DEMs along the four strips (see Langridge et al., 2014). Each of the strips was centred around the mapped trace of the Alpine Fault, having typical swath widths of 1.5–2 km (750–850 m either side of the Alpine Fault).

From southwest to northeast the four strips cover the following areas:

1. **Hokitika River to Styx River** — a 20.4 km long swath covers the northern end of the central section and overlaps the junction with the northern section of the Alpine Fault, defined by the western tip of the Kelly Fault in the area of the Toaroha and Kokatahi rivers (Figure 2.1).
2. **Taipo River to beyond Lake Poerua** — this 22 km long swath spans part of the southern end of the northern section of the fault including Griffin Creek, the Taipo and Taramakau rivers, Inchbonnie and Lake Poerua. Lake Brunner is immediately northwest of this swath.
3. **Haupiri River to beyond Ahaura River** — a 16 km long swath that stretches from near the Haupiri River to the Nancy River in the northeast. A new paleoseismic study was undertaken on the southwest side of the Ahaura River as part of this project in 2018.
4. **Robinson River to Lake Daniell** — this is the longest of the four swaths at c. 32.7 km in length, stretching from the south bank of the Robinson River to the Lake Daniell area in the northeast. This swath spans across the junctions of both the Fowlers and Awatere faults (with the Alpine Fault), in an area dominated by beech forest cover. Following on from a slip rate study at this site (Langridge et al., 2017), a new paleoseismic study was undertaken along this swath at Calf Paddock on the Maruia River as part of this project in 2016. Also prior to this study, an EQC-funded lake-based paleoseismic study was undertaken at Lake Christabel in 2014, immediately southeast of this swath (Howarth et al., 2016b).

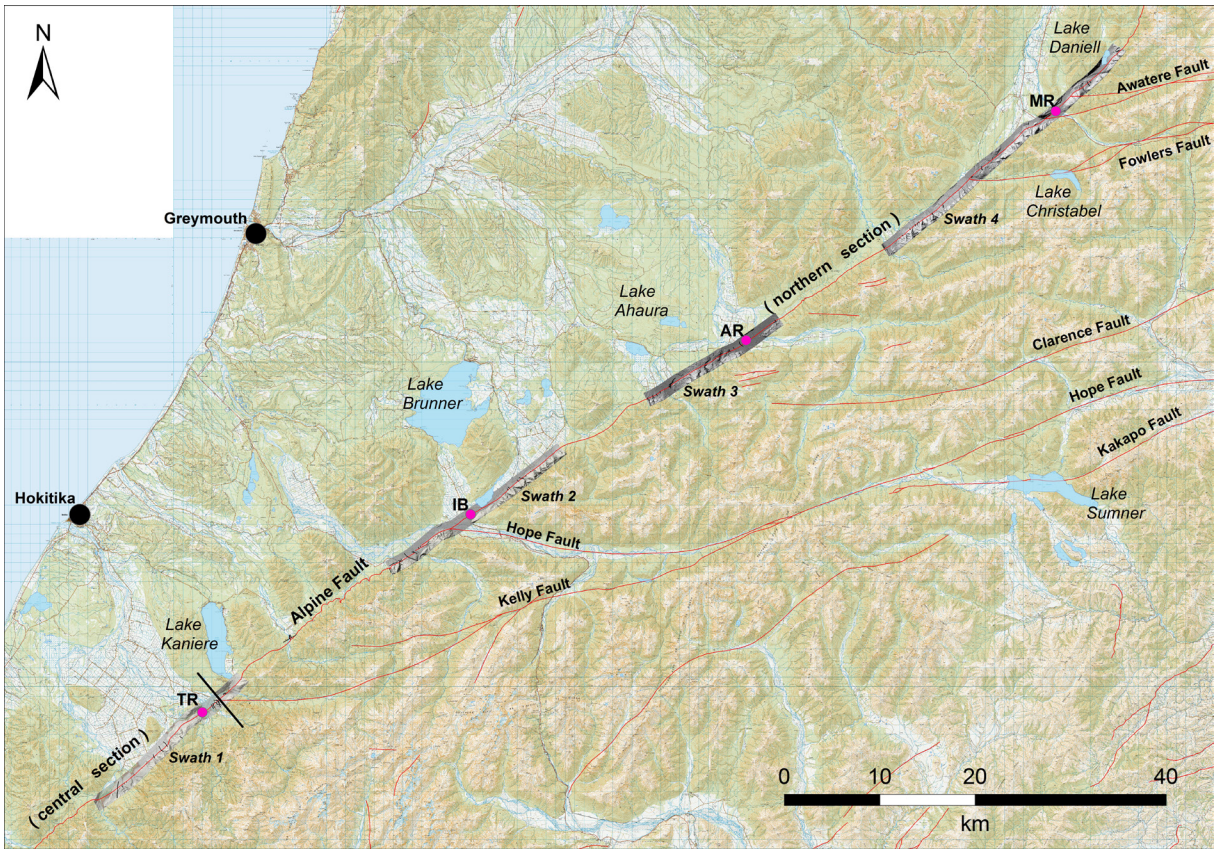

Figure 2.1 Base map of the transition from the central to northern sections of the Alpine Fault (boundary marked by black bar at lower left). LiDAR acquired as part of the NHRP project is shown as 4 swaths, labelled 1–4 from southwest to northeast. Active faults are shown in red. Paleoseismic sites discussed in this report are shown by pink circles at: TR, Toaroha River, IB, Inchbonnie, AR, Ahaura River, and MR, Maruia River. Lakes in this area where paleoseismic histories have been developed are labelled (Kaniere, Brunner and Christabel).

2.2 Mapping on LiDAR-Derived Elevation Models

More detailed mapping of both the main and subsidiary active traces of the Alpine Fault and other faults has been possible where new airborne LiDAR was acquired (Fig. 2.2). These data will be used to update the NZ Active Faults Database (NZAFD; Langridge et al., 2016) and should ultimately supersede GIS line work developed for surface rupture hazard maps for the Alpine Fault (e.g. Langridge and Ries, 2010). We mapped the fault at scales of between 1:4000 and 1:10,000 in a Geographic Information System (GIS). Detailed fault trace mapping assists in understanding the recent history and kinematics of faulting. We have used the LiDAR-derived DEM to map distinctive alluvial surfaces (e.g. Q2a terraces) that are offset across the fault zone, and also structures within the hanging wall block of the Alpine Fault including bedrock faults, foliation, and sackungen (ridge rents). In addition, field sites have been located for paleo-slip studies, and for identification of paleoseismic trench site targets. Examples of LiDAR coverage and maps are presented below, using the Haupiri-Ahaura (Swath 3) and Robinson-Daniell (Swath 4) swaths as examples (e.g. Figures 2.2; 3.1).

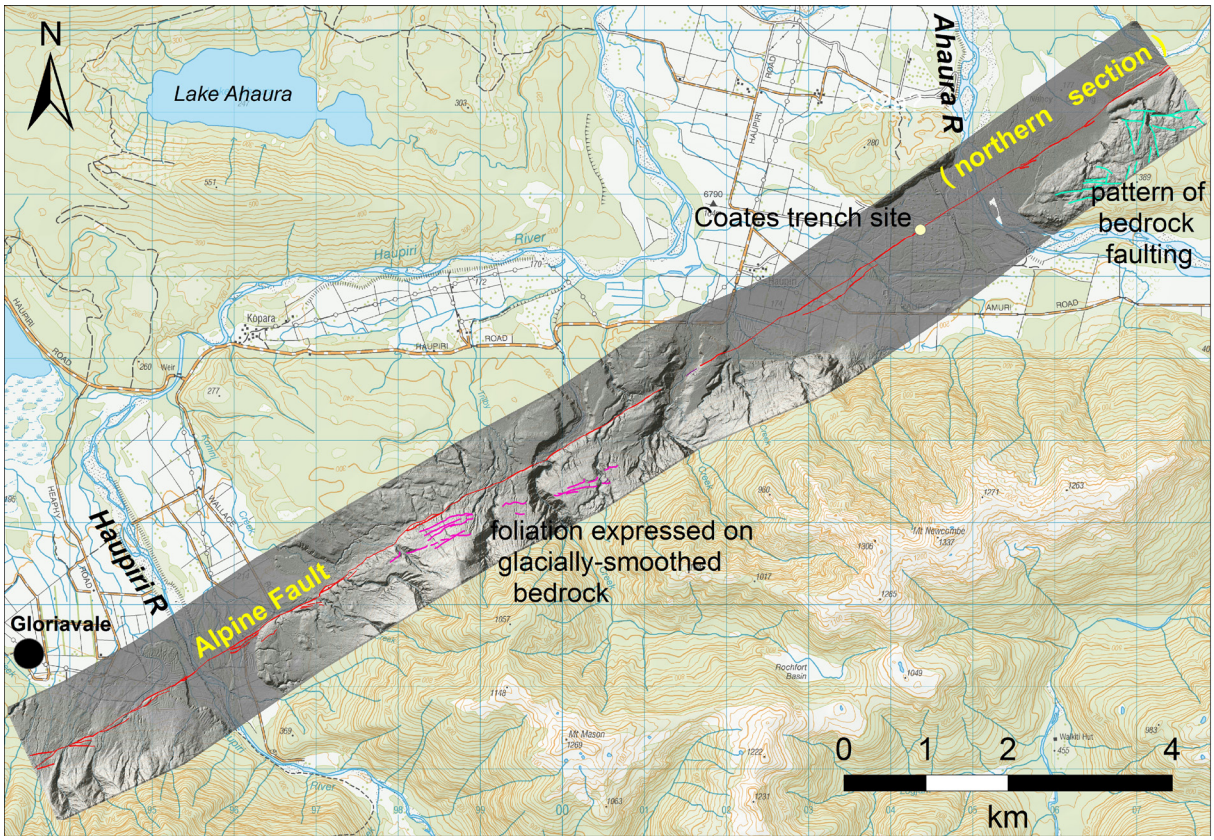

Figure 2.2 Airborne LiDAR swath 3 between the Haupiri and Ahaura rivers. New detailed fault trace mapping (red lines) highlights the Alpine Fault. Bedrock structure in the hanging wall is observed as foliation (pink lines at centre) and bedrock faults with many orientations (blue lines at top right).

3.0 RESEARCH AIM 1.2A — COLLECTION OF ON-FAULT PALEOSEISMIC AND SLIP RECORDS

"We will collect high-resolution paleoseismic records from on- and off-fault sites. We will target on-fault sites where the timing, displacement and number of events can be resolved".

3.1 Calf Paddock (Maruia River) Paleoseismic Site

3.1.1 Introduction

The Calf Paddock (or Maruia River) site is a well-known site along the Alpine Fault due to its ready access, sequence of offset terraces, and because of the presence of a fault creep monitoring wall, built across the fault there in 1964 (Langridge et al., 2017). The site was one of the first recognised places where offset alluvial terraces were used to define the Alpine Fault as active and to assess displacement (Fyffe, 1935; Wellman, 1955; Berryman, 1975). A study by Yetton (2002) was the first to involve excavations at the site. Their permit to excavate was limited to the lowermost faulted terrace adjacent to the river. Results from this terrace highlight that a late Holocene earthquake has faulted that terrace, with a small dextral displacement of c. 1.3 ± 0.3 m, found in combination with a scarp height of c. 0.3 m. The timing of this event has been re-defined by Howarth et al. (2018) as being sometime after AD 1399–1625.

Langridge et al. (2017) excavated four pits on the terraces at the Calf Paddock site, estimating a dextral slip rate of c. 10 ± 2 mm/yr. This study also highlighted that the fault traces had a stepping character through the site, and that the total fault displacement across the terraces peaked at c. 12 m on the second youngest abandoned terrace, rather than across older terraces. These results indicate that there have been at least 2 faulting events on that terrace, where the scarp height is 1.5–2.5 m in height, prior to this study.

3.1.2 Current Study

The scope of the current study was to excavate two new paleoseismic trenches at Calf Paddock in order to assess the evidence for, and date the timings of past earthquakes (Figure 3.1). The site is characterised by a flight of young alluvial terraces that degrade toward the Maruia River. The terraces are offset by the northeast-striking Alpine Fault. Trenches 1 and 2 of this study were excavated across terraces T4 and T2a of Langridge et al. (2017). To aid in this effort, tree coring (dendrochronology) was proposed as a means to obtain a fairly precise minimum age on the timing of the most recent faulting event at the site, which has a mixture of grassland and dense beech forest cover across it.

3.1.3 Maruia Trench-1

Trench-1 was excavated across a c. 3 m high, northwest-facing scarp. The trench is c. 23 m long and on average c. 1.8 m deep. Trench-1 was sited close to a pit (#1) excavated on the hanging wall side of the fault by Langridge et al. (2017) to log and date the alluvial terrace stratigraphy. Therefore, it was possible to correlate the stratigraphy of Trench-1 to Pit 1.

The stratigraphy of Trench-1 is characterised by an alluvial sequence of gravels, sand, and silt, overlain by a suite of colluvial deposits that relate to the faulting of the terrace (degradational terrace t4) after its abandonment. The alluvial sequence on the upthrown side

of the fault was different to that on the downthrown side of the fault, which attests in some part to a different depositional record coupled with horizontal fault slip, which is estimated to be c. 10 ± 2 m at this location.

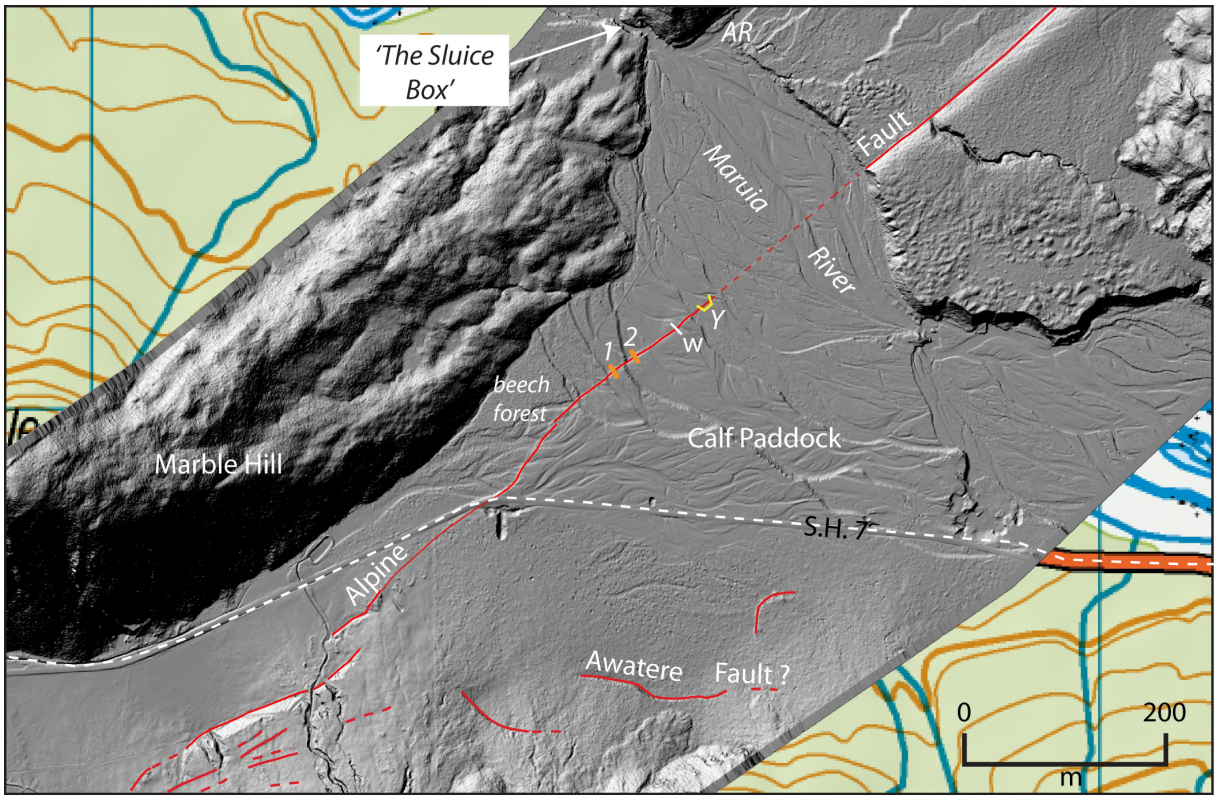

Figure 3.1 Greyscale LiDAR hill-shade strip of the Alpine Fault at Calf Paddock, near Springs Junction. In this area, the northeast-striking Alpine Fault intersects complexly with the ENE-striking Awatere Fault. The Maruia River is met by the Alfred River (AR) at 'The Sluice Box'. Maruia trenches-1 and -2 are indicated by orange bars, the Alpine Fault wall (w), and the Yetton (2002) excavations (Y) are shown by yellow bars.

A summary plot of the stratigraphy of the southwest wall of Trench-1 and the nearby Pit 1, dates and earthquake event horizons is shown in Figure 3.2 as stratigraphic panels. Most of the earthquake event stratigraphy comes from the 'scarp' panel. The most recent earthquake is defined by faulting and bending of older units in the scarp and the deposition of colluvial facies (unit 3c) which drapes across the scarp. The second-to-last or penultimate faulting event is defined by faulting of older units in the scarp that have upward-terminations (fault tips) that underlie colluvial unit 4c, which is interpreted to be a scarp-derived colluvial wedge, i.e. a mixed deposit developed after a surface-faulting event. A possible third event is defined by unit 5c, which may also be a scarp-derived colluvial unit. An older event (IV?) is defined by an angular unconformity (change in dip) within gravelly units on the upthrown side of the fault. As a check of consistency, the same history of paleoseismic faulting and deformation can be extracted from the northeast wall of the trench.

While the stratigraphy in the trench was good, the potential for dating these events was poor. We found few macroscopic pieces of charcoal in the field. Extensive sieving from bulk sediment samples yielded some fine- to very-fine grained charcoal. Some of the samples yielded modern (i.e. post-bomb) radiocarbon ages. Currently, we only have two relevant radiocarbon dates from Trench-1; samples MAR-T1-3(2) and MAR-T1-5, giving ages of 511 ± 18 and 250 ± 55 radiocarbon years BP, respectively. This paucity of dates and also the nature of the dated material, limit our interpretations to this point. Therefore, we aim to submit 2–3 more samples from this trench in order to get better earthquake timing data. The timing of events will be discussed in Chapter 5.

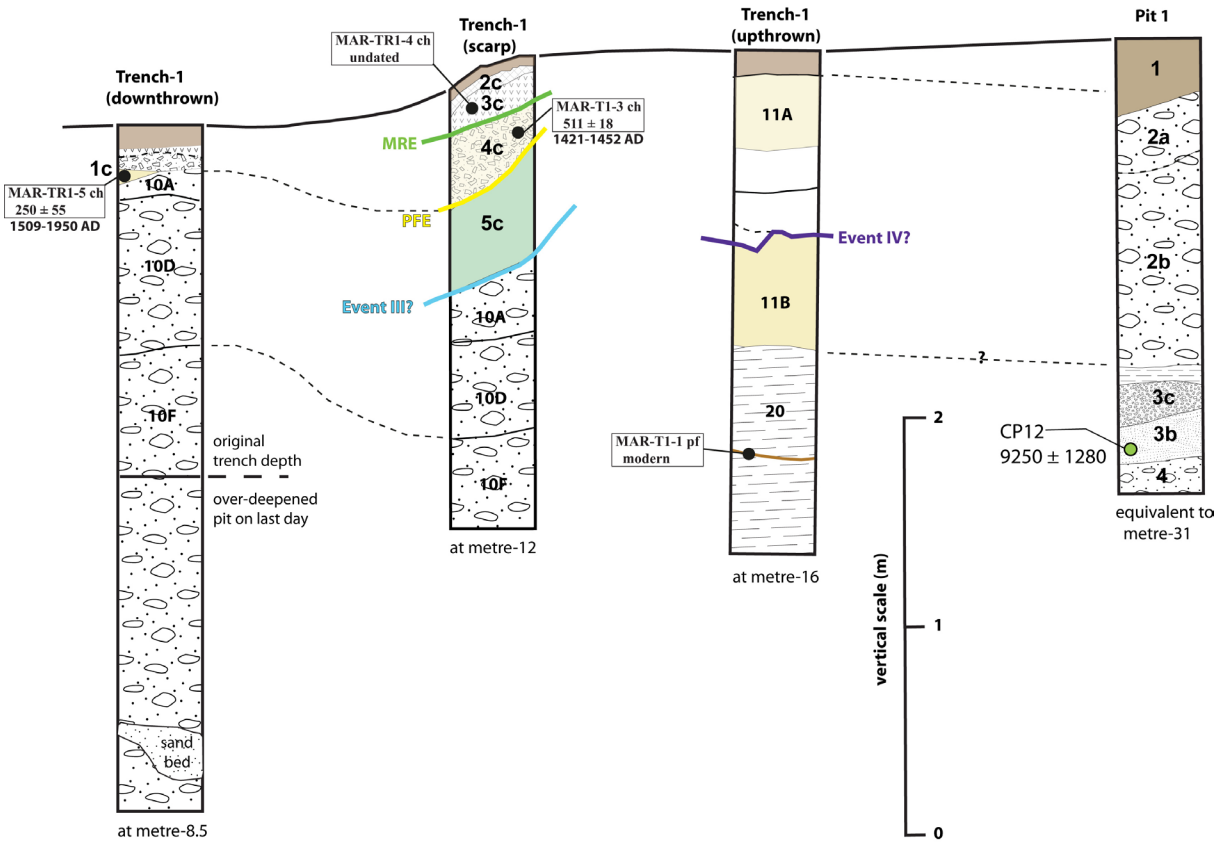

Figure 3.2 Panel diagram showing the stratigraphy, chronology and event history of the southwest wall of Maruia-1 trench (reverse view) and nearby Pit 1. Scarp morphology is indicative. Radiocarbon dates are shown in boxes. Earthquake event horizons, the stratigraphic location of past earthquake events, are shown by coloured lines: MRE - most recent earthquake; PFE - penultimate faulting event, etc. The average depth of the trench was c. 1.8 m.

3.1.4 Maruia Trench-2

Maruia Trench-2 was excavated across a c. 2.8 m high, northwest-facing scarp c. 47 m northeast of Trench-1. Trench-2 is c. 17 m long and up to 1.8 m deep on average. It was sited c. 88 m WSW of Pit 0, which was excavated near the fault monitoring wall by Langridge et al. (2017). Therefore, it was possible to broadly correlate the stratigraphy of Pit 0 across to Trench-2. The trench exposed two major faults zones in the scarp, c. 4–5 m apart.

As with the stratigraphy of Trench-1, Trench-2 was characterised by an alluvial sequence of gravel, sand, and silt, overlain by a suite of colluvial deposits that relate to the faulting of the terrace (degradational terrace T2a) after its abandonment. The lowermost deposits (units 15 & 20) exposed at the base of the trench are comprised of minor sand, silt and pebble gravel beds (Fig 3.3). Unit 15 beds, in the upthrown panel, are planar. In contrast, in the upper scarp panel between the two faults zones, unit 20 beds are juxtaposed against each other by faulting and soft-sediment deformation. Unit 20 deposits are probably truncated by alluvial processes and overlain by 1–1.6 m of sandy cobble to boulder gravel. In Figure 3.3, these gravels are labelled from left to right units 2 and 4 (Pit 0), units 10 and 11 (upthrown block), unit 10 (upper scarp) and unit 30 (lower scarp). These units are probably correlatives, however, age constraints on them across the T2a surface are poor at present. A single radiocarbon date from Pit 0 constrains the age of finer-grained beds in this sequence (Langridge et al., 2017). This allows the possibility that units 3a/3b correlate broadly with units 10s and 10 in the trench. In other words, the thickest exposed gravel section is in the upthrown panel and thus finer beds (10s) may be correlative to other finer, intra-gravel beds.

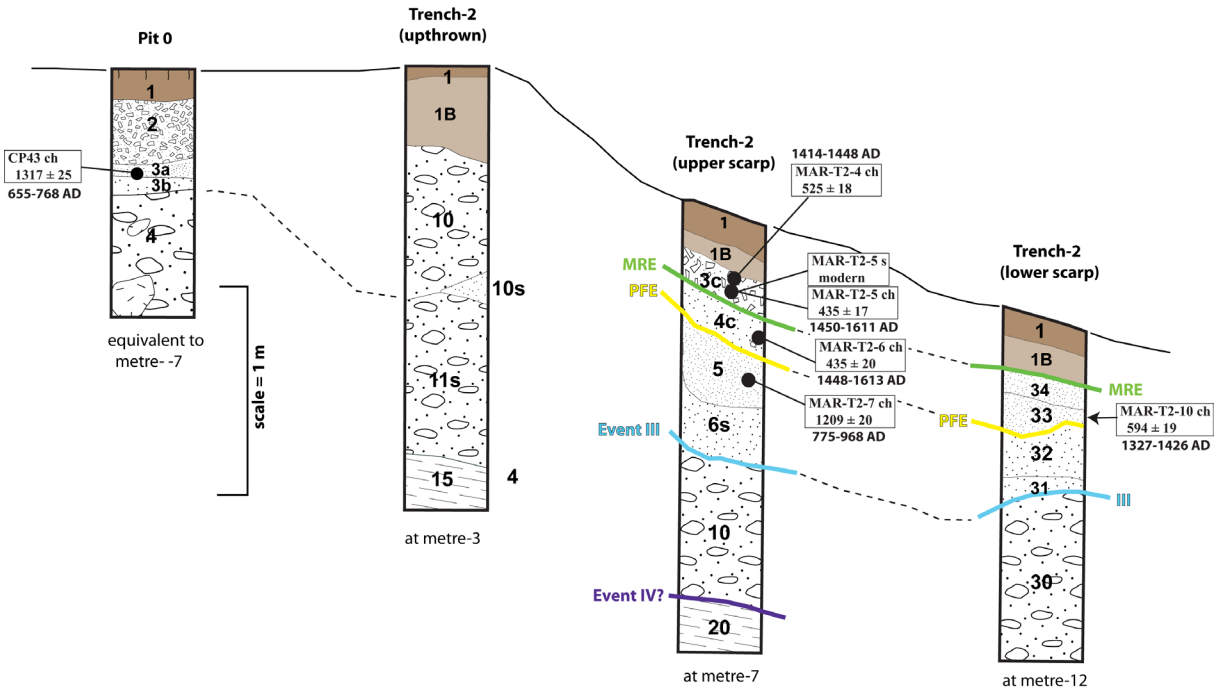

Figure 3.3 Panel diagram showing the stratigraphy, chronology and event history of the southwest wall of Maruia-2 trench and nearby Pit 0. Scarp morphology is indicative. Radiocarbon dates are shown in boxes. Earthquake event horizons - the stratigraphic locations of past earthquake events are shown by coloured lines: e.g. MRE, most recent earthquake; PFE penultimate faulting event. The average depth of the trench was c. 1.8 m.

These alluvial floodplain deposits are overlain by fine-grained alluvial and colluvial deposits that relate to the event stratigraphy in Trench-2. Units 5, 6s, 32 and 31 overlie alluvial gravel in the upper and lower scarp panels (Fig. 3.3). These are interpreted as “low stream power” alluvial deposits, i.e. they were deposited by minor stream flow following abandonment of the terrace. These deposits thicken toward and into the lee of the scarps formed along the two fault zones. These deposits may relate to a back edge and scarp-parallel trough that would have formed adjacent following the termination of gravel deposition across terrace T2a. A charcoal sample from within unit 5 yields an age of 1209 ± 20 radiocarbon years BP. These fine-grained alluvial deposits (units 5, 6, 31, 32) are overlain by colluvial deposits and soils.

Direct correlation of the units, and therefore the paleoseismic events from the upper to the lower fault zone is equivocal, however, we present here the most obvious correlations (e.g. units 5 & 6 to units 31 and 32). In the upper scarp panel units 4c and 3c are defined as scarp-derived colluvial deposits.

The record of paleoseismic event timings for Maruia Trench-2 and their relationship to Maruia Trench-1 will be briefly discussed in Chapter 5. Current age models for these events should be considered preliminary until all of the radiocarbon dating targets have been analysed.

3.1.5 Tree Coring

Tree coring (dendrochronology) was undertaken at the Calf Paddock site because we anticipated that there would be issues with finding datable organic material with which to constrain the timing of the most recent earthquake event there, based on the lack of charcoal found in previous studies (e.g. Langridge et al., 2017). Figure 3.1 shows an area of beech trees between the new Maruia trenches and State Highway 7. In this area the main trace of the Alpine Fault occurs not across grassy terraces but within the beech forest at the foot of Marble Hill. The objective with coring trees in this area was primarily to test the age of the

forest in this area, where surface rupture and/or very strong shaking could have damaged trees or caused them to fall. Colonisation by cohorts of young trees is a known phenomenon after natural disturbances in the forest, such as by earthquake (Wells et al., 1999; Cullen et al., 2003).

Ten tree cores were extracted from nine Red Beech (*Nothofagus fusca*) trees along or near the trace of the Alpine Fault at Calf Paddock. The trees were quite large with diameters of 0.44–0.85 m. Based on growth data from a large population of *N. fusca* sampled along the Hope Fault (Langridge et al. 2007), these trees could range in age from 100–300 years in age. The trees did not show particular signs of stress in the form of tilted trunks or broken crowns, so it is possible that they have grown up from the forest floor along the fault since the last earthquake.

Tree rings from these cores will be counted by Dr. Jonathan Palmer (University of New South Wales, Sydney), but have so far not been analysed. We expect that the outcome of tree ring counting will be a suite of preliminary ages for the timing of forest establishment at the Calf Paddock site. These will be considered along with the results of paleoseismic event timings from the trenches, and the timings of turbidite deposition in the nearby Lake Christabel sediment record (Howarth et al. 2016b).

3.2 Ahaura River (Coates) Paleoseismic Site

3.2.1 Introduction

The remote Ahaura River site is located at Coates farm at Haupiri, 29 km east of Lake Brunner (Figure 2.1). The potential of the site and the two-stranded character of the fault there was first recognised during a reconnaissance by Berryman (1975). A previous paleoseismic study was undertaken on Coates farm by Yetton et al. (1998), who excavated a trench close to the location of the Coates-2 trench (Figure 3.4). Their trench was excavated into the toe of a frontal scarp adjacent to ‘Coates Creek’ and exposed evidence for a single paleoseismic event, constrained by two minimum radiocarbon ages. The timing of this event has been re-defined by Howarth et al. (2018) as being sometime after AD 1642–802.

The scope of the current study was to excavate two new paleoseismic trenches at Coates farm in order to assess the evidence for, and date the timings of past earthquakes, and to relate these to fault displacement there (Figure 3.4). The Coates site is characterised by a progressively abandoned river braid plain (of the Ahaura River), cut across by the northeast-striking Alpine Fault. According to the farmer (Murray Coates), the area was flooded during the 1968 ‘Wahine’ storm, which knocked down a great deal of native forest across the area that is now intensively operated as a dairy farm.

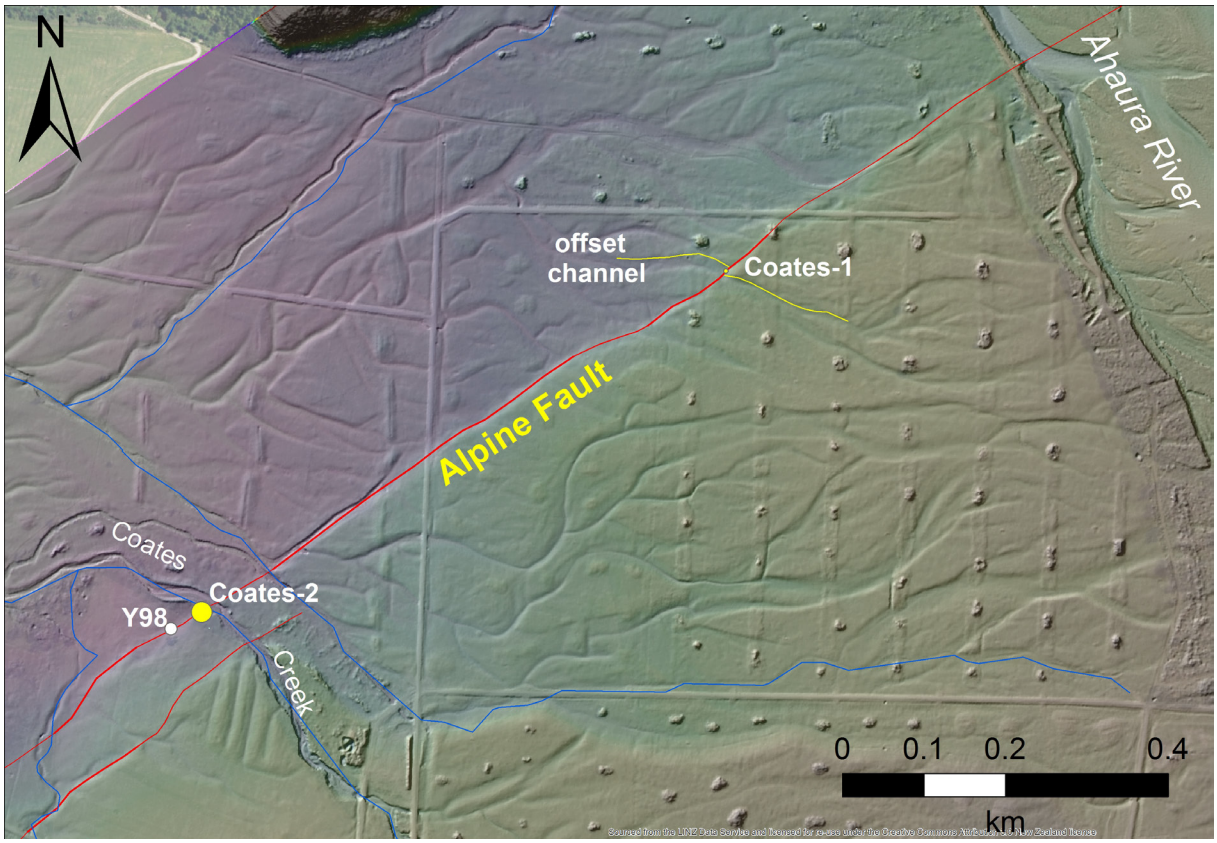

Figure 3.4 A colour DEM shaded model of the Alpine Fault at Coates farm, Haupiri. In addition to the northeast-striking fault traces, the LiDAR hill-shade illustrates several natural (terraces, braid channel) and man-made (farm roads, lumpy gridded windthrow piles) geomorphic features. Coates-2 trench and the Yetton et al. (1998) (Y98) is indicated at lower right, where the Alpine Fault has two distinct traces. The Coates-1 site is highlighted by an offset channel (marked by yellow line).

3.2.2 Geomorphology and Displacement Data from LiDAR

The LiDAR hill-shade map shows an impressive alluvial landscape where the Ahaura River has progressively changed course toward its current NNW path across the Alpine Fault (Figure 3.4). At some previous time, the Ahaura River flowed directly westward to join the Haupiri River, obliquely across the fault, as shown by the relatively fresh geomorphology of a braided river bed. This avulsion may have occurred in two distinct phases here, as the river shows some evidence that it may have still partially flowed around the emergent scarp of the Alpine fault and flowed to the west and NNW. Near the Coates-2 trench site the LiDAR DEM indicates geomorphology that is smoother and more elevated compared to the braid plain (where our Coates-1 trench was sited). This area possibly represents an earlier river bed of the Ahaura River that has been blanketed by finer-grained sheet-flow deposits, related to overbank deposition of the river, or flood material from Coates Creek which cuts across this surface.

Detailed mapping on LiDAR allowed for the recognition of individual offset features. The best example of this is the offset channel which was recognised c. 0.5 km southwest of the Ahaura River (Figure 3.4). We recognised that this site (Coates-1) was a good excavation target because it was associated with a known displacement on the fault. At Coates-1, reverse dextral motion on the Alpine Fault has displaced a braid channel of the former river

floodplain. The abandoned surface is vertically displaced by c. 1.5 ± 0.5 m (down-to-the-northwest). Field observations indicate that the braid channel cut into this surface is offset right-laterally by c. 10 ± 1.5 m at the Coates-1 site[1]. Further, a projection of the current channel thalweg across the fault yields an estimate of 4.5 ± 0.5 m dextral. These data suggest that the c.10 m offset is probably made up of more than 1 earthquake displacement at this site.

A third measure of displacement comes from the reconstruction of a channel fill deposit from the wall of the Coates-1 trench. This deposit is a dish-shaped medium brown silty gravel (with a channel edge cutting laterally up against underlying gravels and silt units), that is truncated by the fault zone in the south wall of Coates-1 trench. This unit does not appear in the north wall of the trench. This unit could be a colluvial deposit shed off the scarp. However, the makeup of this deposit is more in keeping with a cobbly channel, as is observed within the current waterway. We believe the origin of the matrix comes from washing of silt, soil and organic forest detritus into the channel and deposited within the channel cut. A reconstruction of this channel would have its axis on the upthrown side of the fault, separated from the channel axis on the downthrown side of the fault (defined with the trench) of c. 5.5 ± 0.5 m dextral.

3.2.3 Coates-1 Trench

The Coates-1 trench was excavated across the trace of the Alpine Fault between the channel on the upthrown (southeast) side of the fault and the offset riser on the northwest side of the fault. The trench was c. 14 m long and typically up to 1 m depth (Figure 3.5).

The stratigraphy of the trench was characterised by a fining-upward alluvial sequence. The trench is floored with a coarse, sandy cobble to boulder gravel (unit 20), associated with the former braid plain of the Ahaura River. Unit 20 gravels are overlain by medium to fine sandy layers (unit 10) that drape over them. These are interpreted as overbank deposits related to Ahaura River flood events. Unit 10 sands have been largely truncated from the south wall of the trench. However, on the north wall of the trench, these units are thicker and have been preserved in the lee of the scarp, where they appear to have ben folded over and repeated.

The remainder of the stratigraphy is related to the history of the fault following full abandonment of the alluvial surface at Coates-1 (Figure 3.5). Unit 9 is a mixed sandy silty gravel deposit (colluvium) that occurs within the scarp and fault zone of the trench. Clasts within unit 9 comes from gravel unit 20, and its matrix is dominated by orange-brown sand and silt derived from unit 10 and any soil material that was sitting at the ground surface at that time. We interpret unit 9 as a scarp-derived colluvial wedge, that formed after the deposition of units 20 and 10. In the south wall, unit 9 is juxtaposed (across a fault) against another mixed unit (9b). Unit 9b is a dish-shaped medium brown silty gravel (with a channel edge cutting laterally up against underlying gravels and silt units). We interpret unit 9b as a channel fill deposit, probably related to the offset channel at the site. Unit 9b does not appear in the north wall of the trench. This unit could be a colluvial deposit shed off the scarp (or the downslope equivalent of unit 9. However, the makeup of this deposit is more in keeping with an organic-rich cobbly channel, as is observed within the current waterway. We believe the origin of the matrix comes from the washing of silt, soil and organic forest detritus into the

[1] An offset measurement made by back-slipping the LiDAR hill-shade model yields c. 7.5 ± 2.0 m right-lateral slip.

channel and deposited within the channel cut. Unit 9 and 9b are overlain by another mixed unit (8), which is interpreted as a scarp-derived colluvial wedge related to the most recent surface faulting event at the site.

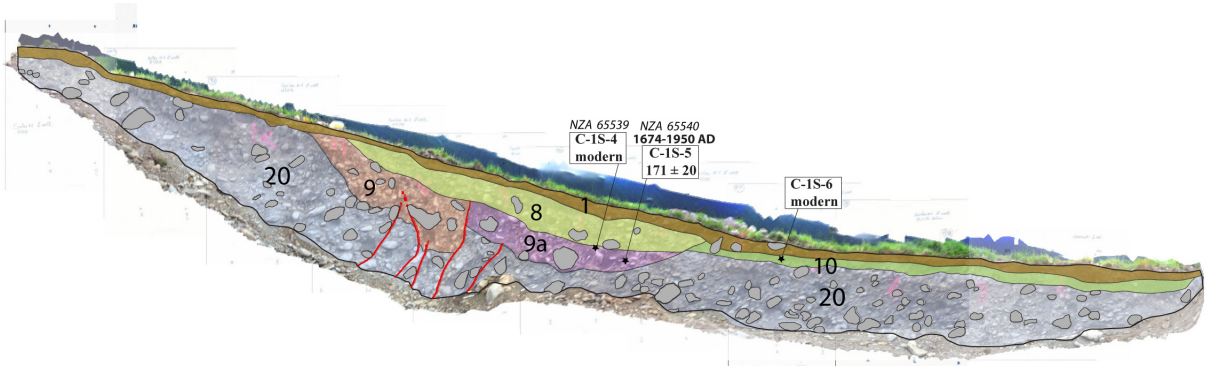

Figure 3.5 Simplified log of the southwest wall of the Coates-1 trench, Haupiri. Faults are indicated by red lines. Units as numbered are described in the text. Radiocarbon dates for this wall are also shown.

A recent soil (unit 1) has formed into the upper deposits in the trench (Figure 3.5). The relationship of this recent soil to the uppermost units is more complicated on the north wall of the trench. In addition to units 8 and 9, mapped on both walls, the north wall has two further units 6 and 7 mapped above unit 8 and beneath the surface soil. Unit 7 is a wedge-shaped unit that is draped over unit 8. Unit 7 is full of degraded wood; some fragments are as large as logs. Unit 7 appears to overlie an organic-rich soil that has formed on top of unit 10 on the north wall. Unit 6 is a mixed colluvial deposit that overlies unit 7 on the north wall of the trench.

Murray Coates alerted us to the fact that this field ('Stoney paddock') had been worked over following the 1968 *Wahine* storm, i.e. undergone dairy farm "terra-forming", as evidenced by the gridded hedgerow piles across this surface. Wood was sampled from the top of unit 10, unit 7, and within unit 6 on the north wall of the trench. All these radiocarbon dates were very young (two were modern), which confirms that the upper stratigraphy was probably related to human farm terra-forming following the 1968 *Wahine* storm. Old aerial photographs allowed us to confirm the change from a bush/forest covered surface as late as at least 1962.

Similar issues were encountered with three radiocarbon dates from units on the south wall of the trench. Two samples dated from the top of unit 9b, and from within unit 10 yielded modern radiocarbon age results. A third sample, from within unit 9b gave a radiocarbon date of 171 ± 20 yr. B.P.

3.2.4 Coates-2 Trench

The Coates-2 trench was excavated across the north-western trace of the Alpine Fault adjacent to Coates Creek (Figures 3.4 and 3.6). The trench was c. 14 m long and typically up to 1 m deep (Figure 3.7). The geomorphology of this location, indicated from the LiDAR hill-shade model, shows an elevated terrace surface with a smooth surface, indicative of a fine-grained cover sequence draped over a gravelly alluvial floodplain sequence (Figure 3.4).

Figure 3.6 View to the southeast of the Coates-2 trench site in the “bull paddock”, Haupiri. The edge of Coates Creek is at left. The digger is about to excavate into and perpendicular to the north-western fault scarp here, which is c. 1.6–2 m in height. The Yetton (2000) trench was sited at the toe of the scarp close to the tree at right.

As at Coates-1, the stratigraphy of the Coates-2 trench was characterised by a fining-upward alluvial sequence (Figures 3.7). The basal trench units are a coarse sandy cobble to boulder gravel (unit 20), which is probably related to an earlier phase of Ahaura River aggradation. Unit 20 gravels are overlain by a cover sequence of finer gravels to silts, which has been variably eroded and deformed from the upthrown to downthrown side of the fault. An extra pit was excavated on the upthrown side of the fault to view the complete, uneroded cover sequence. medium to fine sandy layers that drape over them, interpreted as overbank deposits related to Ahaura River flood events. From youngest to oldest, the planar cover deposits in the trench are numbered 8, 10, 12, 13, 14 and 15. Unit 15 is a dense grey silt that covers gravel unit 20. In places, a transitional (mixed) unit 18 has been mapped to represent that the gravel and silt appear to have been deformed or deposited as a colluvial mixture. Above this the units are predominantly sandy to sandy fine gravels. However, on the downthrown side of the fault two significant cut-and-fill channel units (2 and 4) cut down to near the base of the trench through the planar cover deposits and are filled with medium to fine gravels fining up into gravely sands. Unit2 and 4 channels are seen on both walls and are considered to relate to former scarp-parallel flow of Coates Creek. To support this, we observe that immediately southwest of here, and close to the site of the Yetton (2000) trench, that the fault scarp is slightly curved, as if it had been trimmed by a channel. Units 2 and 8 show subtle evidence in the form of a colour A horizon, of incipient soil development in the top of these units, e.g. unit 8a formed into the top of unit 8. These relations suggest some amount of time has passed to form soils into the top of these deposits, i.e. they may be buried A horizons of former soils. Unit 2 is overlain by a mixed tabular (gravelly sand) unit (1C) that drapes the scarp and grades laterally into a better sorted, possibly alluvial facies of similar material.

Figure 3.7 The northeast wall of the Coates-2 trench showing the stratigraphy on the downthrown side of the fault. The wall is gridded with a 1-m spacing and logged and sampled in detail.

On both walls three main zones of faulting (f1, f2, f3) were recognised cutting through this stratigraphy (Figure 3.7). Fault zone f1 most clearly displaces the basal gravels (unit 20) and terminates up at least as high as unit 10 on the southwest wall. Fault zone f2 cuts up through units 10 and 8 an is truncated against the base of unit 2 channel deposits. One branch of f2 terminates at the base of unit 10. Fault zone f3 is truncated low down in the trench by channel unit 4a. This fault could have potentially cut up higher, but certainly has not been active since the deposition of channel unit 4.

The stratigraphic and structural evidence for three paleoseismic events in the Coates-2 trench is summarised as follows:

- *Most recent faulting event (MRE)* — this event is defined as the upper contact of unit 8 or 8a. Unit 8a is the paleosol formed into unit 8 silts. Unit 8a is in part truncated by erosion, following the most recent faulting event. The event horizon associated with the MRE is overlain by unit 2/2a.
- *Penultimate faulting event (PFE)* — the event horizon associated with the PFE is defined as the upper contact of unit 10 in the trench. In places, on the northeast wall, unit 13 occurs below unit 190, and in this case unit 13 forms the penultimate event horizon.
- *Event III* — Event III is speculative but is defined on the basis of unit 18 on both walls of the trench. Unit 18 has a mixed composition between unit 18 and 20 and it is inferred that it represents a colluvial wedge related to a third (Event III) fault rupture in the Coates-2 trench.

4.0 RESEARCH AIM 1.2B — COLLECTION OF OFF-FAULT PALEOSEISMIC RECORDS

"We will collect high-resolution paleoseismic records from on- and off-fault sites. We will obtain a new high precision record of sedimentation and strong shaking from one lake (Brunner) to augment on-fault paleoseismic data".

4.1 Introduction

A major aim of this project was to build on successful lacustrine paleoseismic studies undertaken at lakes along the central and northern sections of the Alpine Fault, e.g. at lakes Kaniere, Christabel and Rotoiti (Howarth et al. 2016b). Lake Brunner, the largest lake on the West Coast, was the obvious target to undertake new lake coring for paleoseismic studies (Figure 4.1).

Lake Brunner (40 km^2; maximum water depth of 109 m) is a moraine-bounded lake on the West Coast coastal plain, c. 7 km from the trace of the Alpine Fault at Inchbonnie. The lake is fringed by moraines around its northern sector and by large granitic pendants (e.g. Mt Te Kinga) of the Hohonu Range (Suggate, 1965; Nathan et al., 2002), around its flanks. Lake Brunner is fed primarily at present by the Crooked River and by runoff from the Hohonu Ranges, and empties via the Arnold River at Moana (Figure 4.1).

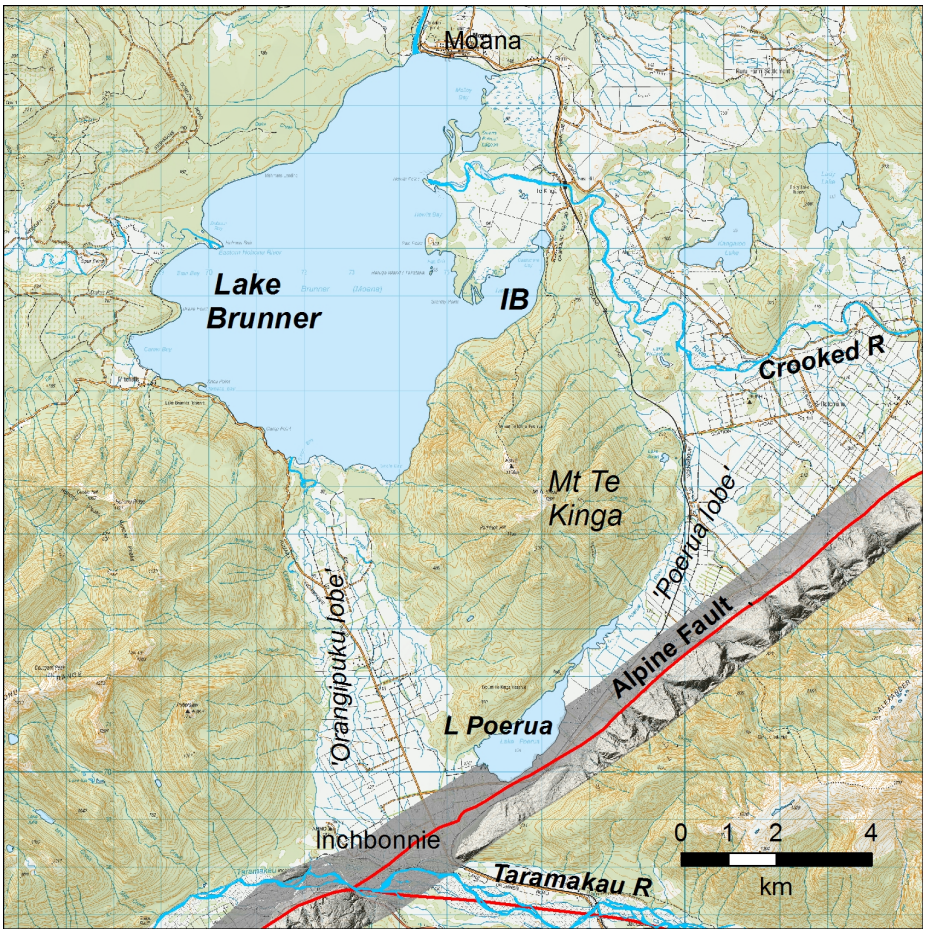

Figure 4.1 Location map of Lake Brunner on the footwall side of the Alpine Fault near Inchbonnie. Lake Brunner core sites are shown as purple dots near the lake depocentre and in Iveagh Bay. The LiDAR hill-shade model tracing the Alpine Fault is part of Swath 2. Lake Poerua and the Taramakau River are at bottom centre. IB, Iveagh Bay.

While it is widely accepted that Lake Brunner was occupied by ice during the last glacial (Suggate, 1965; Barrell et al., 2011), very little is known about the Holocene history of Lake Brunner. The Taramakau River, which is the largest river in this catchment area, has at times during the late Holocene taken three distinct river courses, following the axis of the three glacial lobes related to the Moana moraine sequence (Suggate, 1965; Langridge et al., 2010). Two of these courses (Poerua, Orangipuku) result in the river flowing into Lake Brunner, while the third lobe/course (Taramakau) is the modern course of the river. Based on data from Lake Poerua and its environs, (Langridge et al. 2012) suggest that the last time that the Taramakau River flowed into Lake Brunner was since AD 420 (when the river stopped flowing to the north to the lake) but prior to AD 1230, by which stage a proto-Lake Poerua was forming (and the river was probably flowing to Lake Brunner via the Orangipuku lobe/course) (Figure 4.1).

4.1.1 Site Survey

Approximately 50 km of geophysical lines was collected from Lake Brunner to image the subsurface of its basin floors (Figure 4.2). Geophysical data was collected in 2015–2017 using both a Knudsen 3.5 kHz and 15 kHz central frequency Compressed High-intensity Radar Pulse (CHIRP). The source receiver was mounted on an inflatable boat and towed at least 30 m behind a larger vessel to avoid noise from the outboard motor of the towing vessel. A handheld Global Positioning System (GPS) unit provided positional information for each ping to an accuracy of ± 4 m. Raw data were processed using a band pass and automatic gain control filters in Globe Claritas software, and imported into Paradigm software for visualisation, mapping and interpretation of the subsurface sedimentary features of the lake.

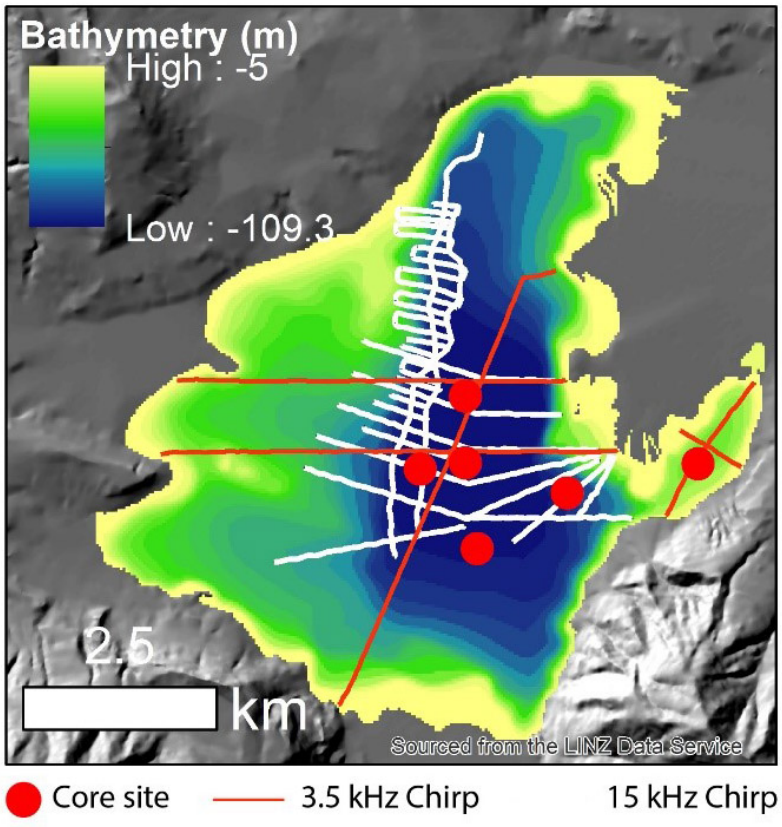

Figure 4.2 The sub-bottom stratigraphy of the lake was surveyed with both 3.5 kHz and 15kHz CHIRP (red and white lines) to identify subaqueous mass-wasting events and the sediments were sampled with 1–6 m Mackereth corer at 6 core sites (red circles).

4.1.2 Sedimentology

A total of fourteen sediment cores, 1–6 m in length, were collected from six core sites along the axis of the lake and in a small sub-basin near Iveagh Bay using Mackereth corers (Mackereth, 1958). Cores were logged visually, Computed Topography(CT)-scanned, and line-scan imaged, and their physical properties (magnetic susceptibility and colour spectrometry) were characterised using a GEOTEKTM multi sensor core logger. Visual core logs and the physical properties data were used to correlate the cores and to identify the different types of deposits in the sediment records. Sedimentary deposits were characterised using grain-size. Grainsize analysis was conducted on a subset of representative deposits that were traced across multiple cores.

4.1.3 Chronology

Chronology for the sedimentary record in Lake Brunner was established by radiocarbon dating 22 terrestrial leaf macrofossils from 5 key sediment cores. The leaves were extracted from deposits formed by background sedimentation. Leaf macrofossils deposited during phases of background sedimentation were targeted because they have proved the most reliable organic fraction for dating in similar lake settings (Howarth et al., 2013). Macrofossils cleaned of residual sediment were subjected to a standard A-A-A (acid-alkali-acid) pre-treatment procedure to remove carbonates, fulvic compounds and humic compounds following the methods of Hua et al. (2001). The pre-treated macrofossils were converted to CO2 by combustion, graphitized and measured by Accelerator Mass Spectrometry (AMS) according to the methods of Baisden et al. (2013) at Rafter Radiocarbon Laboratory.

The radiocarbon dates were calibrated with the SHCal13 calibration curve (Hogg et al., 2013) and integrated with core depth using the P_Sequence prior model with a variable event thickness constant k in OxCal 4.2 to produce an age depth model (Bronk Ramsey, 2008; Bronk Ramsey and Lee, 2013). Core depths were based on a master core from each lake basin that was selected because it provided the most intact stratigraphy. Depth associated with rapidly deposited layers and voids generated by gas were removed from the depth sequence because their formation is near-instantaneous, and they do not represent the passage of time (after Howarth et al., 2012; 2014). The age model was used to derive the timing of turbidites formed by subaqueous mass-wasting using the date function within OxCal. For further details of the chronology methods and use of OxCal models see Howarth et al. (2016b).

4.1.4 Preliminary Results

Previous studies of lakes along the Alpine Fault, including lakes Ellery, Paringa, Mapourika, Kaniere and Christabel, indicate that there are cycles of deposition recorded in the floor of their basins that appear to correspond with major impacts in the catchment (e.g. Howarth et al., 2012, 2013, 2016a, b). The sedimentary archives of these Westland lakes are characterised by four lithofacies: layered silts, type 1 rapidly deposited layer (RDL), type 2 RDL and type 3 RDL (Howarth et al., 2012; 2014; 2016; 2018, Table 4.1).

Table 4.1 Description and interpretation of facies found in cores from Lake Brunner.

Lithofacies	Unit	Description	Classification*	Interpretation
Layered silt	L_2	20–1000 mm thick beds characterized by two units. L_1: 2–50 mm of units coarse-to-medium silt that has relatively high autochthonous organic content. L_2: 2–50 mm units of planar bedded, coarse to medium silt that have low organic content derived from terrigenous sources.	N/A	Formed by gradual accumulation of pelagic (L_1) and terrestrial (L_2) sediment.
	L_1			
Type 1 RDL	D_m	20–1000 mm thick beds of fine sandy gravels and/or deformed lacustrine sediments. Invariably overlain by type 2 RDL	D_{m-2}	Debrite formed by deposition of subaqueous debris flow sediments.
Type 2 RDL	T_1	Up to 400 mm thick beds characterized by three distinct units. T_1: up to 100 mm thick basal unit of massive or planar bedded, medium sand to very coarse silt. T_2: 20–300 mm thick intermediate unit of massive, weakly normally or ungraded, coarse silt that thickens towards the basin centre. T_3: up to 100 mm thick, massive medium silt cap.	T_A to T_{B-2}	Turbidite formed by deposition from high density turbidity currents and associated turbulent suspension clouds formed by basin wide failure of lake deltas and slope sediments.
	T_2		T_{E-2} and/or T_{E-3}	
	T_3		N/A	
Type 3 RDL		Very fine sandy silt that normally grades into medium silt both of which contain terrigenous organic material. Always found interbedded with L_2 beds.	T_{E-2}	Hyperpycnites formed by hyperpycnal flows generated by discharge of sediment laden fluvial effluent.

*Sediment density flow classification from Talling et al. (2012).

The lake records discriminate between two thresholds of earthquake strong ground motions based on lithofacies assemblages that record different landscape responses (Howarth et al., 2014; 2016; 2018). Modified Mercalli Intensity (MMI) 9 shaking is recorded as a type 2 RDL formed by subaqueous mass-wasting, immediately followed by an increase of terrigenous sediment flux from earthquake-induced land-sliding on catchment hillslopes recorded as a stack of type 3 RDL and L2 inorganic silts. MMI 7 shaking is recorded by an isolated type 2 RDL formed by subaqueous mass-wasting, because insufficient terrestrial land-sliding is triggered to produce a sedimentary response in the lake basins. Six MMI 9 and three MMI 7 shaking event were identified in the Lake Brunner record (Figure 4.3). The timing of these lacustrine events is presented and discussed in Chapter 5.

At core depths of 3–5 m, as also seen from geophysical images, is a dramatic transition to more inorganic deposition. We interpret this change in the cores to the presence of a sequence of fluvial deposits related to the influx of sediment from the Taramakau River, which occurred c. 1500 yr. ago in the cores from Lake Brunner.

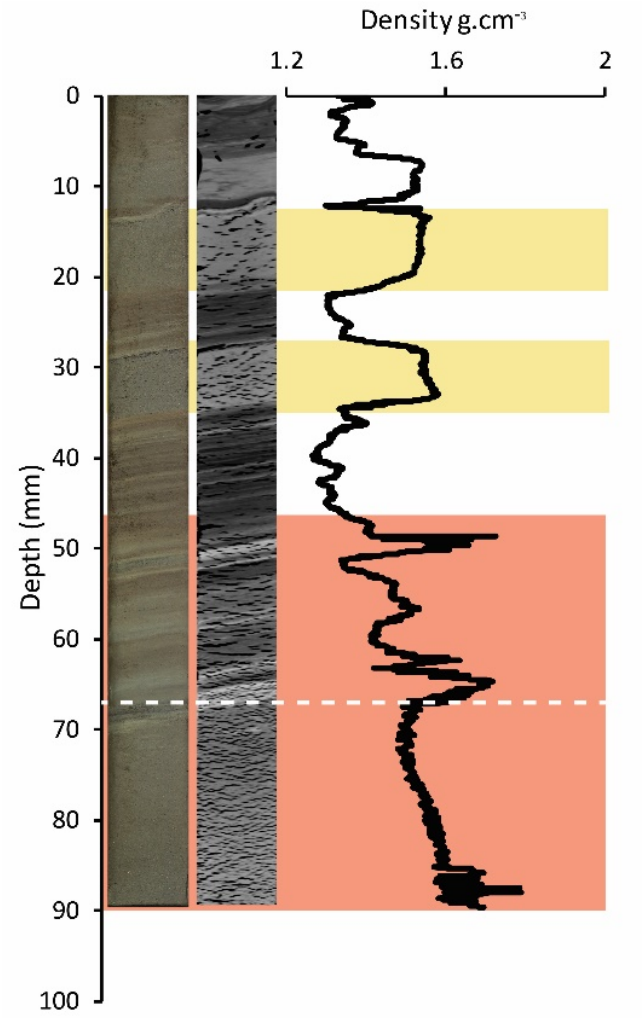

Figure 4.3 Example of core stratigraphy from Lake Brunner from the upper 1 m of the depo-central core sites (BR6m1), showing reconstructed MM 9 (Red) and 7 (yellow) shaking events. The white dashed line demarks the boundary between the subaqueous mass-wasting derived type 2 RDL and interbedded type 3 RDL and L2 inorganic silts that records increased terrestrial sediment flux.

5.0 DEVELOPING ROBUST PALEO-EARTHQUAKE CHRONOLOGIES

"We will undertake a program of high-resolution AMS radiocarbon dating at the Rafter Radiocarbon Laboratory in order to precisely bracket the timing of each paleo-earthquake. We will use OxCal radiocarbon ordering methodologies to develop robust statistical models for paleo-earthquake ages. In addition to those histories from trench sites this will enable a new high precision record of sedimentation and strong shaking from Lake Brunner."

5.1 Introduction

The purpose of undertaking paleoseismic studies is to develop a record of past earthquake timings from stratigraphic and chronologic constraints. On-fault paleoseismic data from sites along the Alpine Fault typically yield the structural evidence for past earthquake ruptures, and these can be related to dextral fault slip where linear markers exist across the fault. However, the chronology of these events is often poorly constrained due to either: a lack of datable material (e.g. due to oxidation of carbon from 'open' gravelly alluvium); and/or the poor quality of carbon found in trenches (e.g. wood or charcoal that has residence time in the geologic environment). In contrast, the timing of subaqueous mass wasting events in lakes can be precisely dated due to the preservation of macro-organic fragments in sediment cores. The following is a summary of the event evidence from the two trench sites and from Lake Brunner.

5.2 Paleoseismic Events in the Maruia-1 Trench

The timing of paleoseismic events in the Maruia-1 trench is currently only constrained by two radiocarbon dates and inferences from luminescence dates at the Calf Paddock site. Further samples yet to be submitted could help constrain the timing of events. The estimates of the timing of faulting events described below come from an OxCal model. In most cases, we use a historical AD 1840 constraint in the OxCal models as there is no evidence for historical faulting along this part of the Alpine Fault.

- *Most recent faulting event (MRE)* — this event is defined by faulting and bending of older units in the scarp and the deposition of colluvial facies (unit 3c) which drapes across the scarp. If we assume that the MRE occurred since the deposition of the younger of the two radiocarbon dates[2] (i.e. sample MAR-TR1-5; Conventional Radiocarbon Age, CRA, 250 ± 55 years before present, yr. BP), then the timing of the MRE was since AD 1483 and up to AD 1840. While this result is poorly constrained it is consistent with the revised estimate for the timing of the MRE from the Yetton (2002) trench, as revised by Howarth et al. (2018), i.e. since AD 1399–1625.

[2] We have evidence from the Maruia-2 trench that charcoal of the age of the older date from the Maruia-1 trench occurs in both the penultimate and Event III colluvial wedges.

- *Penultimate faulting event (PFE)* — this event is defined by faulting of older units in the scarp that have upward-terminations (fault tips) that underlie colluvial unit 4c. Unit 4c is interpreted to be a scarp-derived colluvial wedge, i.e. a mixed deposit developed after the penultimate surface-faulting event. Sample MAR-TR1-3; CRA 511 ± 18 yr. BP), provides a maximum age for the timing of this event as it comes from within unit 4c. Thus, a maximum modelled age for the PFE in this trench is AD 1426–1607. The OxCal model indicates that there have been two faulting events since c. AD 1426 and up to AD 1840.
- *Event III* — this faulting event is defined by the presence of a colluvial unit (5c), deposited across the lee of the scarp. We believe unit 5c to be a scarp-derived colluvial wedge unit, i.e. a mixed deposit formed after a surface-faulting event. The date from unit 4c provides a minimum age for this event. The only other age constraints on this event (and Event IV) come from luminescence dates from Pit 0 (CP41; 1340 ± 190 yr. BP) and Pit 3 (CP32; 1800 ± 160 yr. BP) (Langridge et al., 2017, unpublished data). In this case, we use the date from Pit 0 (combined with a radiocarbon date from the same horizon; CRA 1317 ± 25 yr. BP) to provide a maximum age for the timing of Event III. This yields a modelled timing of AD 754–1486 for Event III in this trench.
- *Older? Event IV?* — a possible paleoseismic Event IV is defined by an angular unconformity (change in dip) within gravelly units on the upthrown side of the fault. In this case, because we believe that the full degradation of this suite of terraces at Calf Paddock (T6 through T2) occurred during one earthquake cycle, in which the Maruia River switched from flowing toward the southwest, to then flowing through 'The Sluice Box', then the timing of Event IV is bracketed by the dates between Pit 3 excavated into terrace T6 and Pit 0, excavated into terrace T2. Thus, the timing of Event IV falls in the range AD 179–749.

These results suggest that there have been up to 3 paleoseismic events in the last 1087 years (or fewer) and up to 4 paleoseismic events in the last 1664 years (or fewer). This yields a maximum recurrence interval for the last two completed earthquake cycles of c. 543 years, and a maximum recurrence interval for the last three completed earthquake cycles of c. 555 years.

5.3 Paleoseismic Events and Slip at the Maruia-2 Site

The timing of paleoseismic events in the Maruia-2 trench is constrained by up to 6 radiocarbon dates (with positive CRA's) and inferences from luminescence dates at the Calf Paddock site. In future, luminescence samples could better constrain the age of some of the units.

- *Most recent faulting event (MRE)* — this event is defined by the upward-termination of faulting on the upper fault zone within the scarp and the deposition of colluvial facies (unit 3c) across the top of that fault. A similar relationship is observed on the lower fault zone, though the upward termination of the faulting is equivocal in relation to the colluvial units there. In this case, due to the obvious reworking of charcoal close to the fault, if we use the youngest reworked charcoal sample within unit 3c (i.e. samples MAR-TR1-5 & 6), as a maximum constraint on the timing of the MRE, then it yields a range from (since) AD 1517–1843. While this result is poorly constrained it is also consistent with the revised estimate for the timing of the MRE from the Yetton (2000) trench, as revised by Howarth et al. (2018), i.e. since AD 1399–1625.

- *Penultimate faulting event (PFE)* — this event is defined by presence of a faulted and deformed (during the MRE) colluvial unit (4c) which is deposited across the fault scarp. The upper fault zone truncates unit 4c on one side and warps it on the other side of the mapped fault at metre-7 in the trench. Unit 4c is interpreted to be a scarp-derived colluvial wedge, i.e. a mixed deposit formed after the penultimate surface-faulting event. We use a sequence of charcoal ages that obviously have a residence time in the environment (sample MAR-TR2-10, -4 and -6), to define a maximum age for the timing of this event[3]. Thus, a maximum modelled age for the PFE in this trench is AD 1453–1596. The calibrated ages indicate that there have been two faulting events since c. AD 1448, however, the ordering of dates in the OxCal model tends to push the maximum timing of the PFE upward to c. AD 1462.
- *Event III* — Event III is defined by the presence of a sandy trough-filling unit (6c), deposited across the scarp following the end of gravel deposition on terrace T2. We cannot show that unit 6c is a scarp-derived colluvial wedge unit, however, we infer that it formed in the lee of the fault scarp because of a faulting event that preceded its deposition. The date from unit 5 (sample MAR-TR2-7; CRA 1209 ± 20 yr. BP) provides a minimum age for this event. As a maximum age constraint for Event III we use the luminescence dates from Pit 0 combined with radiocarbon date CP43 from the same horizon (Langridge et al., 2017, unpublished data). This yields a modelled age bracket of AD 717–945 for Event III in this trench
- *Older? Event IV* — a possible paleoseismic Event IV is defined by the upward termination of faults in the middle of Trench-2 at the top of unit 20. In this case, because we believe that the full degradation of this suite of terraces at Calf Paddock (T6 through T2) occurred during one earthquake cycle, in which the Maruia River switched from flowing toward the southwest, to then flowing through 'The Sluice Box', then the timing of Event IV is bracketed by the dates between Pit 3 excavated into terrace T6 and Pit 0, excavated into terrace T2. Thus, the timing of Event IV falls in the range AD 213–735.

These results suggest that there have been up to 3 paleoseismic events in the last 1125 years (or fewer) and up to 4 paleoseismic events in the last 1649 years (or fewer), using AD 1840 as the minimum age limit for a known earthquake cycle. This yields a maximum recurrence interval for the last two completed earthquake cycles of c. 563 years, and a maximum recurrence interval for the last three completed earthquake cycles of c. 550 years.

5.4 Paleoseismic Events and Slip at the Coates-1 Site

The timing of paleoseismic events in the Coates-1 trench is currently only constrained by 2 radiocarbon dates, because four of the six samples submitted to Rafter Radiocarbon Laboratory returned modern (-ve CRA) ages. We are waiting on the results from a single luminescence sample from unit 10 on the northeast wall. Therefore, at this time it is not possible to discuss the event timings from the Coates-1 trench with any degree of certainty. Other radiocarbon samples could be submitted in future to better constrain the timing of events. The stratigraphic and structural evidence for three paleoseismic events is outlined below.

[3] These charcoal samples come from colluvial units 3c and 4c, and from unit 33 associated with the lower fault zone.

- *Most recent event* — recognised by the presence of colluvium unit 8 on both walls, and the juxtaposition of units 9 and 9b on the south wall (Fig. 3.5).
- *Penultimate faulting event* — recognised by the presence of colluvium unit 9 on both walls. This deposit has a mixture of unit 20 gravel clasts and unit 10 sand and silt, so must have occurred after the deposition of that silt. We currently have an IRSL sediment sample from unit 10 under analysis at the UCLA Luminescence Laboratory. This will provide a bracketing age for the penultimate faulting event at this site. Alternatively, there may be other radiocarbon samples that are still to be selected for dating.
- *Event III?* — A third paleoseismic event is postulated on the basis of the presence and preservation of the unit 10 sands within a fold in the lee of the scarp on the north wall of the trench. The sands must have been folded during the penultimate faulting event, because they are overlain by colluvial unit 9, and are not folded further. We infer though, that these sands could have been deposited in the lee of a scarp that formed prior to their deposition. We cannot tell whether the unit 10 sand cover the entire area of the "Stoney paddock" terrace, however, it seems feasible that these lower energy sand units were deposited in the small fault-parallel basin that formed as a consequence of the scarp forming and from the initial offset of the braid channel on that floodplain. In other words, unit 10 exists most extensively in the small rectilinear area between the riser and the fault where we trenched on the downthrown side of the fault. This provides inferential evidence of a third paleoseismic event that predates the deposition of unit 10. The timing of this event can only be constrained from the IRSL luminescence sample from unit 10 which is currently under analysis.

The offset channel at the Coates-1 site provides some measure of the single-event displacement (SED). If we assume that the channel was offset in 3 displacement events, as inferred from the discussion above, then the single-event displacement is best described by the average of 10 ± 1.5 m, i.e. c. 3.3 ± 1 m dextral. The channel geomorphology is not sensitive enough to be able to pick out individual SED values. The alternative history of the channel is that it was displaced by only two surface rupture events. In this case the mean SED is c. 5 ± 1 m dextral. The total vertical across the surface adjacent to the channel is c. 1.3 ± 0.3 m.

5.5 Paleoseismic Events in Coates-2 Trench

At this point, 11 samples have been dated from the Coates-2 trench. Four of these samples returned modern (-ve CRA) radiocarbon dates. The high number of modern dates, particularly in the uppermost units has given us cause to re-think the stratigraphic and structural relations in the trench. This is especially true because we now know that the site was under forest until probably AD 1968, after which time, the Coates dairy farm was expanded. Therefore, at this point it would not be useful to present a paleoseismic record from the available data. The stratigraphic and structural evidence for three paleoseismic events is outlined in section 3.2.4.

The record in the Coates-2 trench could be improved with further radiocarbon dates. In addition, a third potential trench site has been recognised, c. 250 m to the southwest on the other, parallel trace of the Alpine Fault. We recognise the need to excavate a trench across this second trace to get a complete picture of the paleoseismic record at this location.

5.5.1 Lake Brunner Paleoseismic Record

Ages for the six MMI 9 shaking events in the Lake Brunner record were constrained by ^{137}Cs dating and 22 radiocarbon dates on terrestrial macrofossils using age depth modelling in OxCal 4.2 (Figure 5.1). The most recent MMI 9 shaking event has a 95% highest probability density function (95% HPDF) range of AD 1751 to AD 1586 (Figure 5.2). The dominant mode in the PDF correlates to the timing of the AD 1717 earthquake and we infer that the AD 1717 earthquake on the Alpine Fault was the cause of the most recent MMI 9 shaking event recorded in Lake Brunner. Unfortunately, the lower bound of this event is currently only constrained by one radiocarbon date, which contributes to the poor precision of the event age. On-going work is focused on better constraining the age of the most recent MMI 9 event by increasing the density of radiocarbon dates below this event.

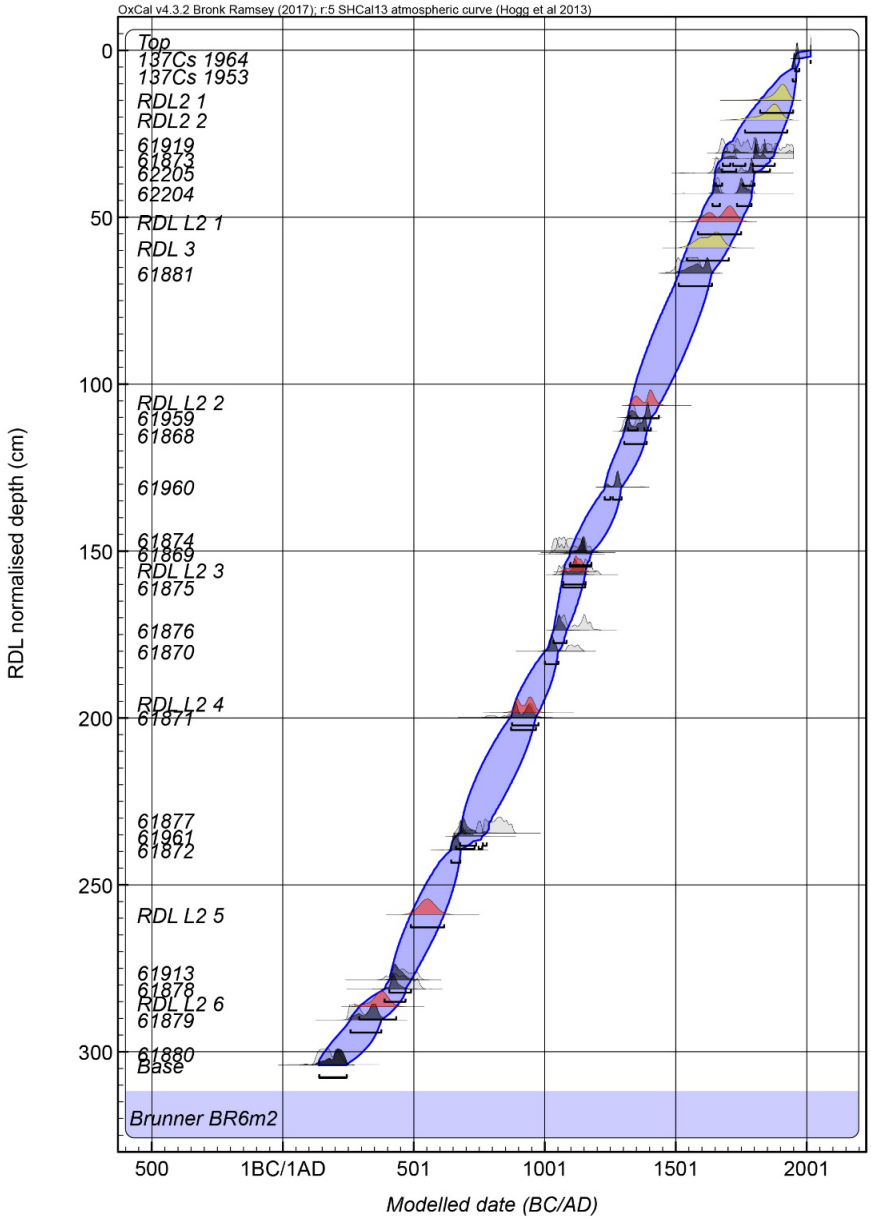

Figure 5.1 Chronological model for Lake Brunner. Chronological models are based on the radiocarbon and ^{137}Cs dates, the SHCal 13 calibration curve (Hogg et al., 2013), and the P_sequence algorithm in OxCal (Bronk Ramsey, 2008). The figure shows the calendar age likelihood (light grey) and posterior probability density functions (PDFs) (dark grey), as well as the age model at the 95% level of confidence (light blue). Rapidly deposited layer (RDL) normalised core depth is the depth of the core with deposits such as turbidites removed. Red PDFs represent the timing of MMI 9 shaking events and yellow PDFs represent the timing of MMI 7 shaking events at the Lake Brunner site.

The age model also constrains the timing of five additional MMI 9 events to AD ~1400, AD ~1125, AD ~925, AD ~550 and AD ~350 (Figure 5.1). We do not report 95% HPDF age ranges for these events because the age model is currently being refined with additional radiocarbon dates. Once completed and combined with existing lacustrine paleoseismic records from lakes Mapourika, Kaniere and Christabel the Lake Brunner chronology will allow the spatial and temporal pattern of rupture to be reconstructed for the northern section of the Alpine Fault. From this it should be possible to establish robust recurrence statistics and conditional probabilities for this fault section.

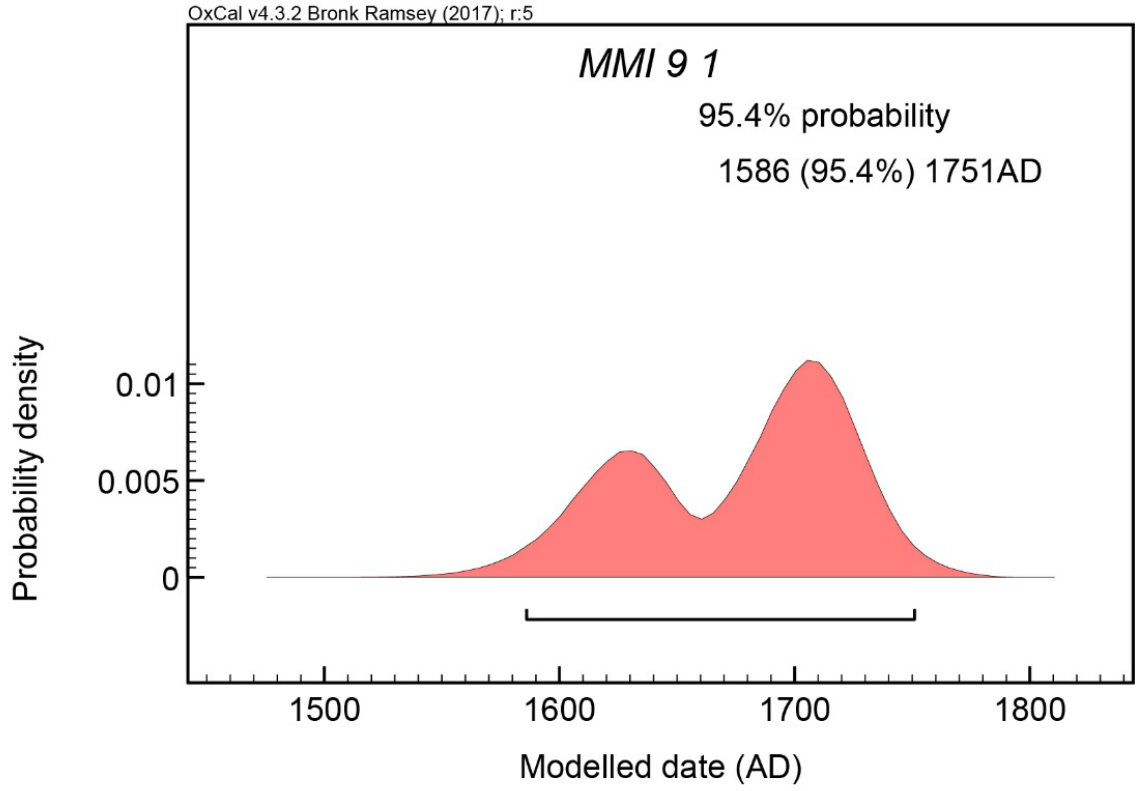

Figure 5.2 Probability density function for the timing of the most recent Modified Mercalli Intensity 9 in Lake Brunner.

6.0 CONDITIONAL PROBABILITY ESTIMATES AND EARTHQUAKE RUPTURE SCENARIOS

> *"Probability estimates will be derived from the longest paleo-earthquake records in lakes along the northern and central sections of the Alpine Fault. Research outcomes will be used to inform us about the behaviour of past earthquake ruptures and future hazard scenarios. An in-house workshop will be held to discuss the implications of our research"*

Conditional Probability (CP) estimates have not been determined at this time, because our interpretations and conclusions are incomplete to date. We plan to work closely with Dr. Glenn Biasi, from the U.S. Geological Survey (Pasadena) to develop CP's as our datasets mature. Our team has already worked closely with Dr. Biasi on Alpine Fault problems and we have a solid record of science publication together (Berryman et al., 2012a, b; Biasi et al., 2015; Clark et al., 2103; Cochran et al., 2017). Dr. Biasi visited New Zealand in 2017 to discuss this project as part of an EQC-funded Alpine Fault workshop run by Dr. Howarth at GNS Science, Wellington on 25 October 2017. We will hold a review workshop in early 2019 at GNS Science, Avalon.

7.0 STAKEHOLDER ENGAGEMENT

> *"Progress reports and scientific papers will be produced in a timely fashion as research comes to fruition. A public lecture series involving the centres of Westport, Greymouth and Christchurch will be used to inform and in turn encourage community preparedness for the next Alpine Fault earthquake(s)."*

Stakeholder engagement and reporting formed an important part of this project. We summarise the work in these areas comprising:

1. Engagement and Outreach
2. Reporting
3. Presentation of scientific papers at conferences
4. Publication of scientific papers
5. Media engagement
6. Scientific conference and field trip
7. A public talk tour

7.1 Stakeholder Engagement and Outreach

The following talks were presented to the wider Civil Defence community which includes Lifelines, Police, Fire, Medical, Health, and Welfare stakeholders as part of the rollout of Project AF8 to the six South Island Civil Defence regions. These talks discussed the hazard posed by the Alpine Fault and its effects on the wider community as part of two 1-day AF8 workshops:

- 8 February 2017 — West Coast Region Civil Defence group, Tai Poutini Polytech, Greymouth.
- 17 February 2017 — Marlborough Region Civil Defence Headquarters, 4 Wither Rd, Blenheim.

Representatives of West Coast Civil Defence — regional and district Emergency Management Officers Chris Raine (West Coast region), Allan Wilson (Grey District), and Kerri Anne Rakena (Buller) visited the Maruia River trench excavations on Thursday, 28 January 2016 to understand how Alpine Fault trenching is undertaken (Fig. 7.1).

The previous day a student group from the University of Canterbury's "Study Abroad" program visited the trench site during field studies (Fig. 7.1). The group was led by Prof. Jarg Pettinga. The students represented a cross-section of visiting geology students from the USA and New Zealand. We delivered a discussion on the preliminary observations in the trenches.

Figure 7.1 Stakeholder engagement and outreach at the Maruia River trench site, January 2016. A. Civil Defence Emergency Management Officers (EMOs) visiting the trench site. B. Study Abroad students learning about paleoseismic trenching at the site of Maruia-1 trench.

7.2 Conference Papers and Presentations

The following conference paper was written and presented as a talk at the 8th international PATA Days Workshop, Blenheim, in November 2017 (in italics):

Howarth, J.D.; Langridge, R.M.; Fitzsimons, S. 2017. Review of existing on-fault paleoseismic data for the North Westland section of the Alpine Fault. In: Clark, K.J.; Upton, P.; Langridge, R.M.; Kelly, K.; Hammond, K.A.T. Proceedings of the 8th International INQUA Meeting on Paleoseismology, Active Tectonics and Archeoseismology: handbook and programme, pp. 154–157.

This conference paper is a prelude to the decadal review paper on Alpine Fault paleoseismic studies (see Howarth et al. 2018 below).

The following abstracts have been submitted to, or have been presented at conferences, followed by a brief statement of their content (in italics):

Howarth, J.D.; Fitzsimons, S.; Langridge, R.M.; Cochran, U.A.; Clark, K.J.; Biasi, G. 2017. Spatio-temporal patterns of rupture during great earthquakes on the Alpine Fault, New Zealand. p. 31 IN: Kelly, K.; Christophersen, A.; Rhoades, D.A.; Gerstenberger, M.C.; Wang, T.; Harte, D.S.; Hammond, K.A.T. 10th International Workshop on Statistical Seismology, 20–24 February 2017, Wellington, New Zealand. Programme and abstracts. Lower Hutt, N.Z.: GNS Science. GNS Science miscellaneous series 101.

This talk was a review of the recent rupture history of the Alpine Fault to date including new lessons being developed as part of this NHRP-funded northern Alpine Fault project.

Langridge, R.M.; Howarth, J.D.; Ries, W.F.; Cochran, U.A.; Villamor, P.; Sagar, M.W. 2016 Earthquake slip, slip rate and paleoseismicity of the Alpine Fault at Calf Paddock, Buller District. p. 43 IN: White, J.D.L.; Smillie, R.W. Geosciences 2016: Annual Conference of the Geoscience Society of New Zealand, 28 November–1 December 2016, Lake Wanaka Centre, Wanaka: abstract volume. Wellington, N.Z.: Geoscience Society of New Zealand. GSNZ miscellaneous publication 145A.

This abstract presented preliminary results from the trenching of the Alpine Fault at the Maruia River site (talk withdrawn from GSNZ due to the Kaikōura earthquake response, November 2016)

Ries, W.F. Langridge, R.M., Howarth, J.D. Cochran, U.A., Thomson, J. 2016. Pulling the plug: Alpine fault triggered river capture and degradation history at the Maruia-Alfred river junction, Buller district. IN: White, J.D.L.; Smillie, R.W. Geosciences 2016: Annual Conference of the Geoscience Society of New Zealand, 28 November–1 December 2016, Wanaka: abstract volume. Wellington, N.Z.: Geoscience Society of New Zealand. GSNZ miscellaneous publication 145A.

This poster described the rapid alluvial degradation history of the Maruia River at Calf Paddock (poster withdrawn from GSNZ because of the Kaikōura earthquake response, November 2016)

Langridge, R.; Howarth, J.; Villamor, P.; Fitzsimons, S.; Cochran, U.; Ries, W.; Strong, D.; Sagar, M. 2018. Reconciling on-and off-fault paleoseismic records for the northern section of the Alpine Fault near Springs Junction. Submitted to: Geosciences 2018: Annual Conference of the Geoscience Society of New Zealand, 27 November–30 November 2018, Napier: abstract volume. Wellington, N.Z.: Geoscience Society of New Zealand. GSNZ miscellaneous publication 149A.

This presentation replaces the cancelled GSNZ 2016 talk with updated science that has been undertaken on the Maruia River and EQC-funded Lake Christabel datasets.

7.3 Published Scientific Papers

The following scientific papers have been published in scientific journals during this project, followed by a brief statement of their content (in italics):

Langridge, R.M.; Ries, W.F.; Dolan, J.F.; Schermer, E.R.; Siddoway, C. 2017. Slip rate estimates and slip gradient for the Alpine Fault at Calf Paddock, Maruia River, New Zealand. *N. Z. Journal of Geology and Geophysics, 60 (2): 73–88,* doi: 10.1080/00288306.2016.1275707.

This paper provides a blueprint for the paleoseismic studies that followed it at the Maruia River site. Understanding the slip rate at Maruia River and its relationship to the offsets there establishes how the Alpine Fault sheds slip rate to faults of the Marlborough Fault System.

Howarth, J.D., Cochran, U.A., Langridge, R.M., Clark, K., Fitzsimons, S.J., Berryman, K., Villamor, P., Strong, D.T. 2018. Past large earthquakes on the Alpine Fault: paleoseismological progress and future directions. New Zealand Journal of Geology and Geophysics 61 (3): 309–328, doi:10.1080/00288306.20181464658.

This paper provides a decadal review of paleoseismic studies on the Alpine Fault. During the last decade huge advances have been made in locating near- and off-fault paleo-earthquake records and also in radiocarbon-based chronologies, summarised in this paper.

7.4 Media Engagement

An important component of this project was to communicate our results to the general public through media engagement. We undertook a successful field-based media campaign at the Maruia River site during field trenching studies in January 2016.

Joanne Carroll of Fairfax Media visited the trench site to report on the Alpine fault investigations for the online Stuff website. This was reported on in print and online:

https://www.stuff.co.nz/national/76403529/Scientists-hunt-for-clues-about-big-Alpine-Fault-quake

Parts of this online article have been re-used by Stuff more than ten times in concurrent articles on the Alpine Fault, e.g.

https://www.stuff.co.nz/national/82524357/Team-granted-funding-to-plan-response-for-Alpine-Fault-megaquake

Julian Thomson of GNS Science was used throughout the trenching campaign to collect still frame, drone and interview coverage for his GNS blog. This material is summarised at:

http://juliansrockandiceblog.blogspot.com/2016/02/digging-into-alpine-fault.html

A large portion of Julian's material was gifted to Television New Zealand so that a television news story could be developed around the Alpine Fault research being undertaken as part of the NHRP-funded project (Fig. 7.2). Rob Langridge worked with Lisa Davies (TV1 News) to develop a story that was aired the night after the 14 February 2016 M_w 5.7 aftershock in the Christchurch area.

https://www.tvnz.co.nz/one-news/new-zealand/digging-down-into-a-fault-line-to-find-answers

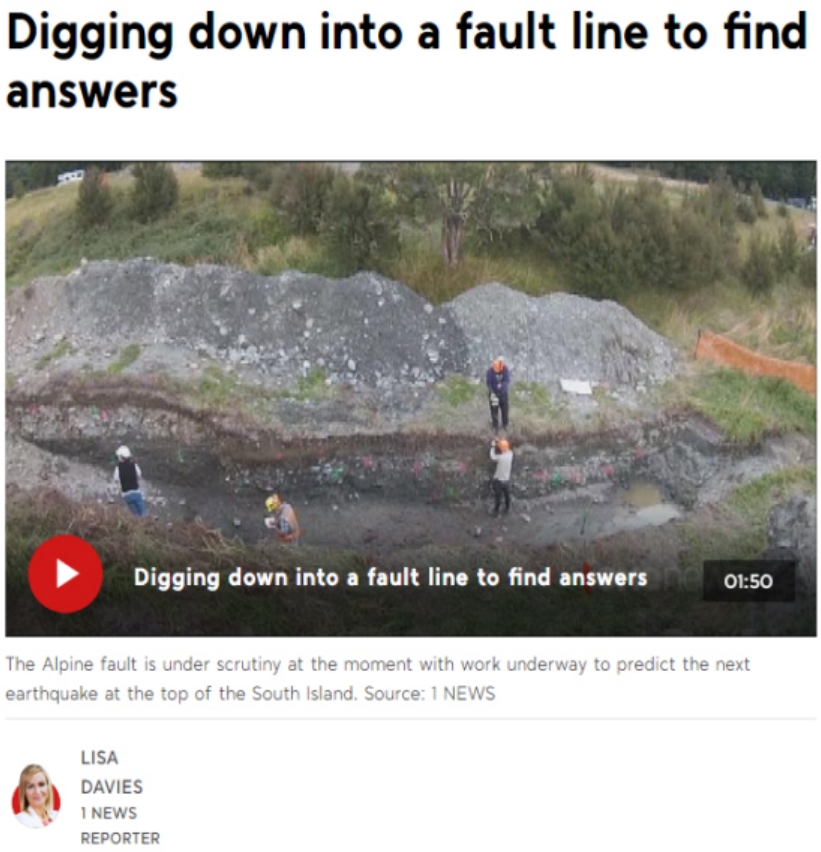

Figure 7.2 Screengrab from the TVNZ News website highlighting the article on Alpine Fault research taking place at the Maruia River site (URL shown above).

7.5 Scientific Conference and Field Trip

The 8th International PATA Days Workshop on Paleoseismology, Active Tectonics, and Archeoseismology (PATA) was scheduled to be held on the West Coast of the South Island in April 2017 to highlight the 300th anniversary of the last great rupture of the Alpine Fault. Due to the occurrence of the November 14 2016 Kaikōura earthquake the 8th PATA Days Workshop was subsequently delayed and moved to the anniversary of the Kaikōura quake, being held in Blenheim from 12–19 November 2017.

Nevertheless, there was a significant component of the Alpine Fault story that we wanted to showcase as part of the meeting. The post-conference field trip, held over three days (17–19 November 2017), included 57 participants from 17 countries. Day 2 of the field trip focused on the Alpine Fault, and in particular its northern section. An important component of the field trip was gaining some critique on our recent scientific results from national experts on the Alpine Fault and international experts in paleoseismology, who were in attendance

Figure 7.3 Day 2 of the South Island field trip held as part of the 8th International PATA Days Workshop, 18 November 2017. A. Rob Langridge describes the late Holocene history of Lake Poerua to PATA Days participants. B. Rob describes the character of the northern section of the Alpine Fault at the Maruia River site.

Day 2 of the field trip progressed from Reefton to Moana and Lake Poerua (Fig. 7.3), and on to a stop along the Alpine Fault within the bush near Inchbonnie. We returned to Lake Brunner (Moana) for lunch and discussed the potential for paleo-earthquake records from lakes. Later that day we visited the Maruia River paleoseismic site and discussed the preliminary results of research there.

The 3-day field trip was reinforced by the production of a field trip guide:

Upton, P., Langridge, R.M., Stahl, T., Van Dissen, R.J., Howarth, J.D., Berryman, K.R., Clark, K.J., Kelly, K., Hammond, K.A.T. 2017. 8th International PATA Days, Blenheim, New Zealand. Three-day post-conference fieldtrip: northern South Island, Alpine Fault and ruptures of the 2016 Kaikoura earthquake, 17–19th November 2017. Lower Hutt, N.Z.: GNS Science. 64 p.

7.6 Public Talk Tour

"The record of past earthquakes and their slip obtained at the transition from the central to northern sections of the Alpine Fault will result in more reliable forecasting of the next great earthquake which in turn will encourage community preparedness"

Based on the success of a Public talk tour following the NHRP-funded Alpine Fault John O'Groats project in 2015 and the conclusion of Dr. Jamie Howarth's Post-Doctoral fellowship, we proposed to run a similar talk tour following the science related to this project.

A public talk tour for this project has been delayed until early 2019 while we await further results. The current plan is to combine this talk tour with the Project AF8 roadshow to be held in the South Island in March/April 2019. We aim to deliver a 3-talk tour with venues in Arahura at the Ngati Waewae marae, at Greymouth (Grey District Council) and in Westport (public talk). These venues reflect our desire to engage with *Iwi* and to speak at venues close to the northern section of the Alpine Fault, where our research results are most relevant. The main speakers will be Dr. Rob Langridge (GNS), Dr. Jamie Howarth (VUW), Dr. Caroline Orchiston (UoO) and one other guest speaker.

8.0 DISCUSSION

8.1 Local Trench Site-to-Lake Record Correlations

On-fault trench sites and lake sites were chosen with a view toward correlating the timing of events from sites that were proximal to one another. For example, the Maruia River site is c. 6 km north of Lake Christabel, and the Lake Brunner site is c. 8 km north of the Inchbonnie and Lake Poerua study sites (Langridge et al., 2010, 2012, 2017; Howarth et al., 2018). Similarly, the Lake Kaniere site, at the junction of the central and northern sections is c. 5 km northeast of the Toaroha trench site (Yetton et al., 1998; Howarth et al., 2018; Langridge et al., in prep). The following describes only the well-constrained results from the Maruia River-Lake Christabel pair of sites. In future when their chronologies are improved, results from the Inchbonnie-Brunner and Toaroha-Kaniere site pairs will be discussed.

8.2 Maruia River & Lake Christabel — Integrated Paleoseismic Event and Slip History

By combining the results of the two trenches from this study with previous trenching at the site by Yetton (2002) the following event chronology can be developed (Figure 8.1). At this point we bring in data from Lake Christabel which was studied as part of an EQC-funded paleoseismic project (Howarth et al. 2016b).

- *Most recent faulting event (MRE)* — occurred since AD 1483 and prior to AD 1840. The displacement associated with this event appears to be small (c. 1–1.6 m dextral) (Langridge et al., 2017). The timing of the most recent "significant mass wasting and sediment flux (SMW&SF) event in the lake occurred between AD 1767 and 1848. The results for the timing of the MRE from the trenching study compare favourably with those from Lake Christabel, especially given the differences in the quality of radiocarbon dating material and subsequent age modelling.
- *Penultimate faulting event (PFE)* — in this case, we use the overlap of the timings of the PFE in both trenches, because in Trench-2, reworking of the charcoal pushes the model beyond its useful limits. The timing of the PFE at Maruia River is between AD 1426 and 1596. The timing of the penultimate SMW&SF event in the lake is tightly constrained to AD 1405–1448. The subsequent overlap between the timing of the MRE from the trenching study and the SMW&SF event from Lake Christabel, is very small and occurs from AD 1426–1448. However, given the difficulties with dating events in the trench, it is preferable to use the timing of this event from the lake (i.e. AD 1405–1448), as characterising the penultimate displacement event on the Alpine Fault at Maruia River.

- *Event III* — For Event III, we also use the overlap of the timings of the event in both trenches. Thus, the combined timing of Event III at Maruia River is between AD 754 and 945. The third major event in Lake Christabel had no significant sediment flux event associated with it and is described as a major significant mass wasting event (SMW) by Howarth et al. (2016b). The timing of this major SMW event in the lake is tightly constrained to AD 940–1005. There is a very small overlap between the age distributions for the trenches and the lake (spanning AD 940–945). However, given the difficulties with dating the deposits in the trench, and the maximum ages that come from charcoal dates, it is preferable to consider the timing of this event from the lake (i.e. AD 940–1005), as characterising the third displacement event on the Alpine Fault at Maruia River.

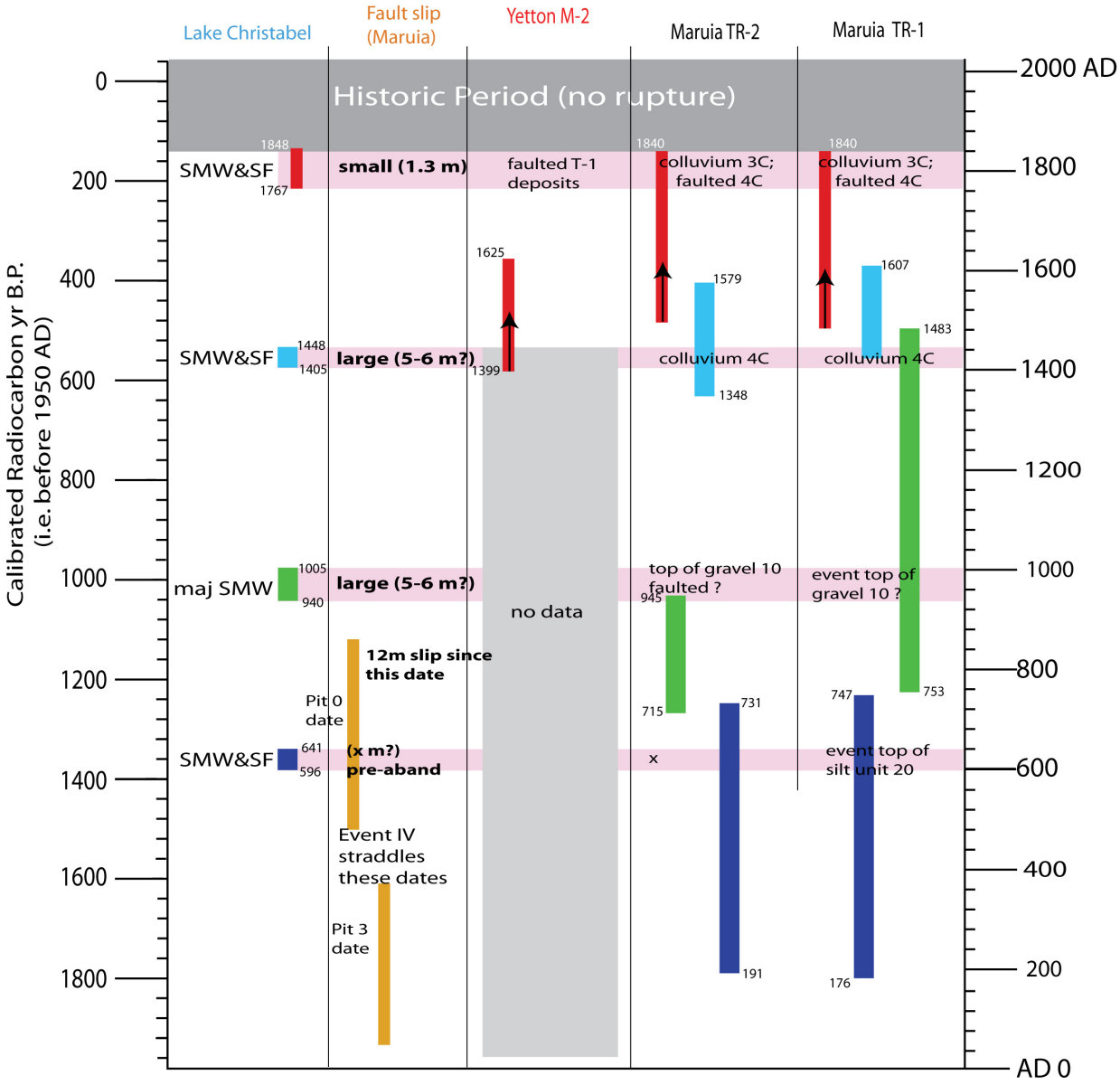

Figure 8.1 Space for time diagram showing on-fault and off-fault paleoseismic records and fault slip for sites in the Springs Junction area. Events are: most recent (red), penultimate (blue); Event III (green, and Event IV (navy blue). At left, precise shaking events recorded in Lake Christabel. SMW&SF, significant mass wasting and sediment flux vs. maj SMW, major significant mass wasting events; centre left, fault slip recorded at Maruia River and two IRSL dates (orange); centre, paleoseismic result from Yetton (2002); at right, timing records from the new trenches at Maruia River.

The PFE and Event III at Maruia River account for most of the 12.0 ± 1.3 m that is measured associated with the suite of offset degraded terraces and their risers, i.e. less the slip accounted for by the MRE. If we simply split the remaining displacement (c. 10.7 m), the single-event dextral displacement for the PFE and Event III were c. 5–6 m each in size.

- *Older? Event IV* — a possible paleoseismic Event IV at Maruia River is mainly constrained by the two IRSL dates from pits 0 and 3 (Langridge et al., 2017). During this time interval it is inferred that the Maruia River was captured by the gap at The Sluice Box and avulsed to form the local set of inset degradation terraces at Calf Paddock.

The overlap of timing between trench-1 and trench-2 given all the other constraints is c. AD 191–731. This age range overlaps with the timing of a third SMW&SF event at Lake Christabel (i.e. AD 596–641), which provides a more precise estimate of the timing of an Event IV? rupture of this part of the Alpine Fault.

The range of maximum inter-event times for the last 2–3 earthquake cycles is 543–563 years from trench studies at Maruia River. By considering the precise age ranges produced for shaking events in Lake Christabel and their relationship to known faulting events at Maruia River it is possible to estimate inter-event times for the northern section of the Alpine Fault in this area. Results from Lake Christabel indicate that there have been up to 2 SMW&SF and one major SMW events in the last 940 years (leading up to AD 1840) and up to 3 SMW&SF and one major SMW events in the last 1244 years. This yields a maximum recurrence interval for the last two completed earthquake cycles of c. 470 years, and a maximum recurrence interval for the last three completed earthquake cycles of c. 414 years.

9.0 CONCLUDING THOUGHTS

An important goal of this project has been to advance our understanding of the paleoseismicity of the northern section of the Alpine Fault. Preliminary data from this project indicate that the approach used for the central and southern sections of the Alpine Fault, as summarised by Howarth et al. (2018) is valid for the northern section of the fault (Figure 9.1). A major success in this study has been unravelling one of the longest on-fault paleoseismic records on the Alpine Fault, at Maruia River, and being able to match event-to-event paleo-earthquake timings and slip against the lake-based paleoseismic record at Lake Christabel (Howarth et al., 2106b).

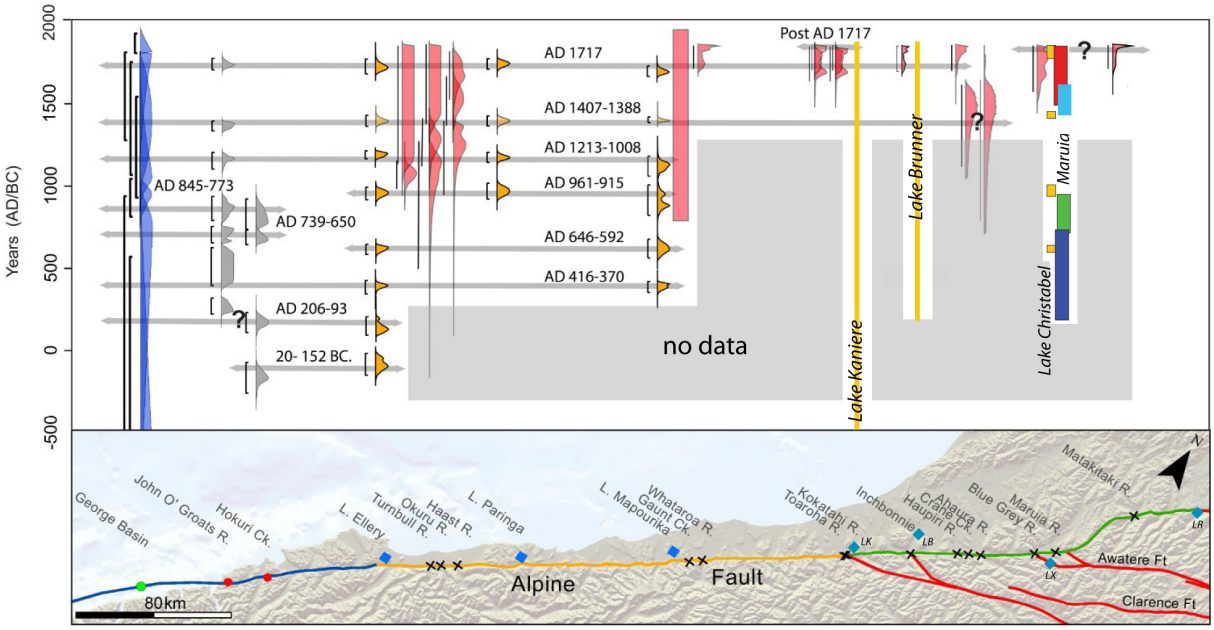

Figure 9.1 Preliminary space for time diagram showing on-fault and off-fault paleoseismic records for sites along the Alpine Fault (modified after Howarth et al., 2018). New data for the northern section is at right, extending event records into the past. Lakes are: LK, Kaniere; LB, Brunner, LX, Christabel, and LR, Rotoiti. Event timing data for Lake Christabel and Maruia River is as shown in Figure 8.1. Event timing data for LK and LB are pending but spans at least the last c. 1800 years.

The potential for unravelling the past rupture behaviour of the Alpine Fault is becoming within reach (Howarth et al., in review). Long (>2000 yr.) off-fault paleoseismic records exist for sites in Fiordland (Berryman et al., 2012b; Cochran et al., 2017) and for lakes such as Ellery, Kaniere and Rotoiti (Howarth et al., 2016a, b, in review). More fruitful and longer on-fault paleoseismic sites are being selected that hold better dating potential (e.g. the Toaroha-Staples and Maruia River sites) (Langridge et al., in review; this study). Without doubt, the record of the timing of, and slip during, past surface-rupturing earthquakes on the Alpine Fault is more complex along the northern section of the fault. While the frequency of earthquakes on the southern and central sections of the fault is quasi-periodic (Berryman et al., 2012b; Biasi et al., 2015; Cochran et al., 2017), the northern section record is complicated by several factors including: 1) a decreasing slip rate along its length from southwest to northeast, perhaps with step-wise drops adjacent to the intersections with faults of the Marlborough Fault System (MFS; Norris and Cooper, 2001; Langridge et al., 2010, 2017); 2) extended ruptures from the central section that overrun the central/northern section boundary; and 3) interactions related to 1 and 2 and the stress changes that are likely imparted to this section of the fault, as it essentially becomes part of the MFS, i.e. the distributed Australia-Pacific plate boundary in northern South Island.

Paleoseismic sites along the Alpine Fault are spaced roughly 40 km apart on average. There is clearly potential to better understand the fault behaviour of the northern section through a densification of both on-fault (e.g. Blue Grey and Robinson rivers) and off-fault lake (e.g. lakes Ahaura and Daniell) sites as well considering non-traditional on-fault paleoseismic sites such as at Camp Creek (Upton et al., 2017). In some cases, sites that have been investigated with shallow trenches or are poorly dated (e.g. Blue Grey and Matakitaki rivers), also need to be re-visited to develop better records. Improved mapping and identification of paleo-slip sites from LiDAR is also an important future target.

This research and supporting work is re-shaping the paradigm of the last few very large (M_W »7) to great (M_W >8) earthquakes on the northern section of the Alpine Fault. Once our datasets are finalised we will be able to show, within the precision of our modelled radiocarbon age distributions, that very long ruptures related to the central section of the fault often continue father to the northeast than the prescribed central/northern section boundary near Lake Kaniere. These inferences come from dated evidence of surface rupture in trenches, e.g. at Inchbonnie, and from the proximity of intense shaking and catchment response local to lakes adjacent to the Alpine Fault, e.g. Lake Brunner.

10.0 ACKNOWLEDGMENTS

We wish to thank landowners for access to land, especially to the Department of Conservation (DoC) for access to both the Calf Paddock area and Lake Brunner. We thank Murray Coates for permission to open trenches on his farm at Haupiri. We also thank Delia Strong, Ursula Cochran, William Ries, Matt Sagar, Pilar Villamor, Lisa Dowling and Julian Garcia-Mayordomo for help in the field. This report was reviewed by Phaedra Upton and Nicola Litchfield and we thank them for their interest and comments.

11.0 REFERENCES

Baisden WT, Prior CA, Chambers D, Canessa S, Phillips A, Bertrand C, Zondervan A, Turnbull J, Kaiser J, Bruhn F 2013. Rafter radiocarbon sample preparation and data flow: accommodating enhanced throughput and precision. *Nuclear Instruments and Methods in Physics Research Section B: Beam Interactions with Materials and Atoms*. 294:194–198.

Barrell DJA, Andersen BG, Denton GH. 2011. Glacial geomorphology of the central South Island, New Zealand. Lower Hutt (NZ): GNS Science. (GNS Science monograph; 27). 2 v.

Barth NC, Toy VG, Langridge RM, Norris RJ. 2012. Scale dependence of oblique plate-boundary partitioning: new insights from LiDAR, central Alpine fault, New Zealand. *Lithosphere.* 4(5):435–448. doi:10.1130/L201.1.

Beavan J, Denys P, Denham M, Hager B, Herring T, Molnar P. 2010. Distribution of present-day vertical deformation across the Southern Alps, New Zealand, from 10 years of GPS data. *Geophysical Research Letters*. 37:L16305. doi:10.1029/2010GL044165.

Berryman KR. 1975. Earth deformation studies reconnaissance of the Alpine Fault. N.Z. Lower Hutt (NZ): New Zealand Geological Survey. 30 p. Report EDS 30.

Berryman KR, Beanland S, Cooper AF, Cutten HN, Norris RJ, Wood PR. 1992. The Alpine Fault, New Zealand: variation in Quaternary structural style and geomorphic expression. *Annales Tectonicae*. VI:126–163.

Berryman K, Alloway B, Almond P, Barrell D, Duncan R, McSaveney M, Read S, Tonkin P. 2001. Alpine Fault rupture and landscape evolution in Westland, New Zealand. In: Böse M, editor. Glaciation and periglacial in Asian high mountains: Proceedings of the 5th International Conference on Geomorphology; 2001 Aug 23–28; Tokyo, Japan. Berlin (DE): Gebrüder Borntraeger.

Berryman K, Cooper A, Norris R, Villamor P, Sutherland R, Wright T, Schermer E., Langridge R, Biasi G. 2012a. Late Holocene rupture history of the Alpine Fault in South Westland, New Zealand. *Bulletin of the Seismological Society of America*. 102:620–638. doi:10.1785/0120110177.

Berryman KR, Cochran UA, Clark KJ, Biasi GP, Langridge RM, Villamor P. 2012b. Major earthquakes occur regularly on an isolated plate boundary fault. *Science*. 336:1690–1993. doi:10.1126/science.1218959.

Biasi GP, Langridge RM, Berryman KR, Clark KJ, Cochran UA. 2015. Maximum-likelihood recurrence parameters and conditional probability of a ground-rupturing earthquake on the southern Alpine Fault, South Island, New Zealand. *Bulletin of the Seismological Society of America.*105(1):94–106. doi:10.1785/0120130259.

Bronk Ramsey C. 2001. Development of the radiocarbon calibration program OxCal. *Radiocarbon*. 43(2A):355–363.

Bronk Ramsey C. 2008. Deposition models for chronological records. *Quaternary Science Reviews*. 27(1–2):42–60.

Bronk Ramsey C, Lee S. 2013. Recent and planned developments of the program OxCal. *Radiocarbon*. 55(2):720–730.

Carpenter BM, Kitajima H, Sutherland R, Townend J, Toy VG, Saffer D. 2014. Hydraulic and acoustic properties of the active Alpine Fault, New Zealand: Laboratory measurements on DFDP-1 drill core. *Earth and Planetary Science Letters*. 390:45–51.

Clark KJ, Cochran UA, Berryman KR, Biasi G, Langridge RM, Villamor P, Bartholomew T, Litchfield NJ, Pantosti D, Marco S, et al. 2013. Deriving a long paleoseismic record from a shallow-water Holocene basin next to the Alpine fault, New Zealand. *Geological Society of America Bulletin*. 125(5/6):811–832. doi:10.1130/B30693.1.

Cochran UA, Clark, KJ, Howarth JD, Biasi GP, Langridge RM, Villamor P, Berryman KR, Vandergoes MJ. 2017. A plate boundary earthquake record from a wetland adjacent to the Alpine fault in New Zealand refines hazard estimates. *Earth and Planetary Science Letters.* 464:175–188. doi:10.1016/j.epsl.2017.02.026.

Cullen LE, Duncan RP, Wells A, Stewart GH. 2003. Floodplain and regional scale variation in earthquake effects on forests, Westland, New Zealand. *Journal of the Royal Society of New Zealand*. 33(4):693–701.

De Pascale GP, Langridge RM. 2012. New on-fault evidence for a great earthquake in 1717, central Alpine fault, New Zealand. *Geology*. 40:791–794. doi:10.1130/G33363.1.

De Pascale GP, Quigley MC, Davies TRH. 2014. Lidar reveals uniform Alpine fault offsets and bimodal plate boundary rupture behavior, New Zealand. *Geology*. 42(5):411–414. doi:10.1130/G35100.1.

DeMets C, Gordon RG, Argus DF, Stein S. 1994. Effect of recent revisions to the geomagnetic reversal time scale on estimates of current plate motions. *Geophysical Research Letters*. 21(20):2191–2194.

Hogg AG, Hua Q, Blackwell PG, Niu M, Buck CE, Guilderson TP, Heaton TJ, Palmer JG, Reimer PJ, Reimer RW, et al. 2013. SHCal13 Southern Hemisphere Calibration, 0–50,000 Years cal BP. *Radiocarbon*. 55(4):1889–1903.

Howarth JD, Fitzsimons SJ, Norris RJ, Jacobsen GE. 2012. Lake sediments record cycles of sediment flux driven by large earthquakes on the Alpine fault, New Zealand. *Geology*. 40(12):1091–1094.

Howarth JD, Fitzsimons SJ, Jacobsen GE, Vandergoes MJ, Norris RJ. 2013. Identifying a reliable target fraction for radiocarbon dating sedimentary records from lakes. *Quaternary Geochronology*. 17:68–80.

Howarth JD, Fitzsimons SJ, Norris RJ, Jacobsen GE. 2014. Lake sediments record high intensity shaking that provides insight into the location and rupture length of large earthquakes on the Alpine Fault, New Zealand. *Earth and Planetary Science Letters*. 403:340–351.

Howarth JD, Fitzsimons SJ, Norris RJ, Langridge R, Vandergoes MJ 2016a. A 2000 yr. rupture history for the Alpine fault derived from Lake Ellery, South Island, New Zealand. *Geological Society of America Bulletin*. 128(3/4):627–643.

Howarth JD, Strong DT, Fitzsimons SJ, Langridge R. 2016b. A revised earthquake history for the North Westland segment of the Alpine Fault. Lower Hutt (NZ): GNS Science. 46 p. (GNS Science report; 2016/27).

Howarth JD, Cochran UA, Langridge RM, Clark K, Fitzsimons SJ, Berryman K, Villamor P, Strong DT. 2018. Paleoseismological progress on the Alpine Fault. *New Zealand Journal of Geology and Geophysics*. 61(3):309–328. doi:10.1080/00288306.2018.1464658.

Howarth JD, Barth NC, Fitzsimons SJ, Richards-Dinger K, Biasi GP, Cochran U, Clark K, Langridge R, Sutherland R (in review). Long earthquake records and computer simulations reveal mode switching between major and great earthquakes on a plate boundary fault

Hua O, Jacobsen GE, Zoppi U, Lawson EM, Williams AA, McGann MJ. 2001. Progress in radiocarbon target preparation at ANTARES AMS Centre. *Radiocarbon*. 43(2A):275–282.

Langridge RM, Berryman KR. 2005. Morphology and slip rate of the Hurunui section of the Hope Fault, South Island, New Zealand. *New Zealand Journal of Geology and Geophysics*. 48(1):43–58.

Langridge R, Duncan R, Almond P, Robinson R. 2007. Indicators of paleoseismic activity along the western Hope Fault. Lower Hutt (NZ): GNS Science. (GNS Science consultancy report; 2006/151).

Langridge RM, Villamor P, Basili R, Almond P, Martinez-Diaz JJ, Canora C. 2010. Revised slip rates for the Alpine fault at Inchbonnie: implications for plate boundary kinematics of South Island, New Zealand. *Lithosphere*. 2:139–152. doi:10.1130/L88.1.

Langridge RM, Ries WF, Farrier T, Barth NC, Khajavi N, De Pascale, GP. 2014. Developing sub 5-m LiDAR DEMs for forested sections of the Alpine and Hope faults, South Island, New Zealand: implications for structural interpretations. *Journal of Structural Geology*. 64:53–66. doi:10.1016/j.jsg.2013.11.007.

Langridge RM, Ries WF, Litchfield NJ, Villamor P, Van Dissen RJ, Barrell DJA, Rattenbury MS, Heron DW, Haubrock S, Townsend DB, et al. 2016. The New Zealand Active Faults Database. *New Zealand Journal of Geology and Geophysics*. 59(1):86–96. doi:10.1080/00288306.2015.1112818.

Langridge RM, Ries WF, Dolan JF, Schermer ER, Siddoway C. 2017. Slip rate estimates and slip gradient for the Alpine Fault at Calf Paddock, Maruia River, New Zealand. *New Zealand Journal of Geology and Geophysics*. 59(2):73–88. doi:10.1080/00288306.2016.1275707.

Langridge RM, Villamor P, Howarth JD, Litchfield NJ, Clark KJ, Sutherland RJ, Ries WF, Sabat F (2018 in review). Paleoseismicity of the Alpine fault at the Toaroha River (Staples site), Westland, New Zealand: Implications of a post-1717 AD rupture event.

Litchfield NJ, Villamor P, Van Dissen RJ, Nicol A, Barnes PM, Barrell DJA, Pettinga JR, Langridge RM, Little TA, Mountjoy JJ, et al. 2018. Surface rupture of multiple crustal faults in the 2016 MW 7.8 Kaikoura, New Zealand, earthquake. *Bulletin of the Seismological Society of America*. 108(3B):1496–1520. doi:10.1785/0120170300.

Mackereth FJH. 1958. A portable core sampler for lake deposits. *Limnology and Oceanography*. 3:181–191.

Nathan S, Rattenbury MR, Suggate RP, compilers. 2002. Geology of the Greymouth area [map]. Lower Hutt (NZ): Institute of Geological and Nuclear Sciences. 1 sheet + 65 p. (Institute of Geological and Nuclear Sciences 1: 250 000 geological map; 12).

Norris RJ, Cooper AF. 2001. Late Quaternary slip rates and slip partitioning on the Alpine Fault, New Zealand. *Journal of Structural Geology*. 23(2/3):507–520.

Norris RJ, Cooper AF. 2007. The Alpine Fault, New Zealand: surface geology and field relationships. In: Okaya DA, Stern TA, Davey FJ, editors. *A continental plate boundary: tectonics at South Island, New Zealand*. Washington (DC): American Geophysical Union. p. 157–175. (Geophysical monograph; 175).

Stirling MW, McVerry GH, Gerstenberger MC, Litchfield NJ, Van Dissen RJ, Berryman KR, Barnes P, Wallace LM, Villamor P, Langridge RM, et al. 2012. National seismic hazard model for New Zealand: 2010 update. *Bulletin of the Seismological Society of America*. 102(4):1514–1542. doi:10.1785/0120110170.

Stirling MW, Litchfield NJ, Villamor P, Van Dissen RJ, Nicol A, Pettinga J, Barnes P, Langridge RM, Little T, Barrell DJA, et al. 2017. The Mw 7.8 Kaikōura earthquake: surface fault rupture and seismic hazard context. *Bulletin of the New Zealand Society for Earthquake Engineering*. 50(2):73–84.

Suggate RP. 1965. Late Pleistocene geology of the northern part of the South Island, New Zealand. Wellington (NZ): Department of Scientific and Industrial Research. 91 p. (New Zealand Geological Survey bulletin; 77).

Sutherland R, Eberhart-Phillips D, Harris RA, Stern TA, Beavan RJ, Ellis SM, Henrys SA, Cox SC, Norris RJ, Berryman KR, et al. 2007. Do great earthquakes occur on the Alpine Fault in central South Island, New Zealand? In: Okaya DA, Stern TA, Davey FJ, editors. *A continental plate boundary: tectonics at South Island, New Zealand*. Washington (DC): American Geophysical Union. p. 235–251. (Geophysical monograph; 175).

Sutherland R, Toy VG, Townend J, Cox SC, Eccles JD, Faulkner DR, Prior DJ, Norris RJ, Mariani E, Boulton C, et al. 2012. Drilling reveals fluid control on architecture and rupture of the Alpine Fault, New Zealand. *Geology*. 40(12):1143–1146.

Talling PJ, Mason DG, Sumner EJ, Malgesini G. 2012. Subaqueous sediment density flows: depositional processes and deposit types. *Sedimentology*. 59 (7):1937–2003. doi:10.1111/j.1365–3091.2012.01353.x.

Tonkin PJ, Basher LR. 1990. Soil-stratigraphic techniques in the study of soil and landform evolution across the Southern Alps, New Zealand. *Geomorphology*. 3:547–575. doi:10.1016/0169-555X(90)90020-Q.

Upton P, Langridge RM, Stahl T, Van Dissen RJ, Howarth JD, Berryman KR, Clark KJ, Kelly K, Hammond KAT. 2017. 8th International PATA Days, Blenheim, New Zealand. Three-day post-conference fieldtrip: northern South Island, Alpine Fault and ruptures of the 2016 Kaikoura earthquake, 17–19th November 2017. Lower Hutt (NZ): GNS Science. 64 p.

Wallace LM, Beavan RJ, McCaffrey R, Berryman KR, Denys P. 2007. Balancing the plate motion budget in the South Island, New Zealand using GPS, geological and seismological data. *Geophysical Journal International*. 168(1):332–352. doi:10.1111/j.1365-246X.2006.03183.x.

Wellman HW. 1955. New Zealand quaternary tectonics. *Geologie Rundschau*. 43(1):248–257.

Wells A, Yetton MD, Duncan RP, Stewart GH 1999. Prehistoric dates of the most recent Alpine fault earthquakes, New Zealand. *Geology.* 27(11):995–998.

Yetton MD. 1998. Progress in understanding the paleoseismicity of the central and northern Alpine Fault, Westland, New Zealand. *New Zealand Journal of Geology and Geophysics*. 41(4):475–483.

Yetton MD. 2000. The probability and consequences of the next Alpine Fault earthquake, South Island, New Zealand [PhD thesis]. Christchurch (NZ): Canterbury University.

Yetton MD. 2002. Paleoseismic investigation of the North and West Wairau sections of the Alpine Fault, South Island, New Zealand. Wellington (NZ): Earthquake Commission. 96 p. EQC Research Report No.: 99/353.

Yetton MD, Wells A, Traylen NJ. 1998. The probability and consequences of the next Alpine Fault earthquake. Wellington (NZ): Earthquake Commission. EQC Research Report No.: 95/193.

Yetton MD, Wells A. 2010. Earthquake rupture history of the Alpine Fault over the last 500 years. In: Williams AL, Pinches GM, Chin CY, McMorran TJ, Massey CI, editors. *Geologically active: delegate papers 11th Congress of the International Association for Engineering Geology and the Environment*; 2010 Sep 5–10; Auckland, New Zealand. Boca Raton (FL): CRC Press.